

1. Report No. FHWA/RD-83/027		2. Government Accession No.		3. Recipient's Catalog No.	
4. Title and Subtitle Design and Construction of Stone Columns Volume II, Appendixes				5. Report Date May 1983	
				6. Performing Organization Code HNR-30	
7. Author(s) R. D. Barksdale and R. C. Bachus				8. Performing Organization Report No. SCEGIT-83-104 (E20-686)	
9. Performing Organization Name and Address School of Civil Engineering Georgia Institute of Technology Atlanta, Georgia 30332				10. Work Unit No. (TRAI) 34H3-012	
				11. Contract or Grant No. DTFH61-80-C-00111	
12. Sponsoring Agency Name and Address Federal Highway Administration Office of Engineering and Highway Operations Research and Development Washington, D.C. 20590				13. Type of Report and Period Covered Final August 1980-August 1982	
				14. Sponsoring Agency Code CME/	
15. Supplementary Notes Project Manager: A. F. DiMillio (HNR-30)					
16. Abstract <p>Stone columns have been used since the 1950's as a technique for improving both cohesive soils and silty sands. Potential applications include (1) stabilizing the foundation soils to support embankments, approach fills and reconstruction work on weak cohesive soils, (2) supporting retaining structures (including Reinforced Earth), bridge bent and abutment structures on slightly marginal soft to stiff clays and loose silty sands, (3) landslide stabilization and (4) reducing liquefaction potential of clean sands. Also, stone columns under proper conditions can greatly decrease the time required for primary consolidation.</p> <p>Volume I describes construction and design aspects of stone columns. This report presents six Appendixes (A-F) which describe various design examples and other pertinent information that supports the main text (Volume I) of the final report.</p>					
17. Key Words Construction Ground Improvement Design Site Improvement Field Performance Specifications Stone Columns			18. Distribution Statement No restrictions. This document is available to the public through the National Technical Information Service, Springfield, Virginia 22161		
19. Security Classif. (of this report) Unclassified		20. Security Classif. (of this page) Unclassified		21. No. of Pages 45	22. Price

APPENDIX A

SELECTED CONTACTS FOR STONE COLUMNS

UNITED STATES

Vibroflotation Foundation Company
600 Grant Street
93th Floor
Pittsburg, Pennsylvania 15219
Phone: 412/288-7676

Mr. Robert R. Goughnour
Mr. Albert A. Bayuk
Mr. James Warren
Mr. George O. H. Reed

GKN Keller, Inc.
6820 Benjamin Road
Tampa, Florida 33614
Phone: 813/884-3441

Mr. Tom Dobson
Mr. Gary Alexander
Mr. Barry Slocombe
Dr. Gerhardt Chambosse

Kencho, Inc.
25030 Viking St.
Hayward, California 94545
(Sand Compaction Piles)

Mr. K. Hayashi
Mr. Tony Sullivan
Mr. Howard West

Note: Toyomenka (America) Inc. were formerly the trading company for the Kensetsu Kikai Chosa Co., Ltd. Vibrators. Kencho, Inc., a division of Kensetsu Kikai Chosa Co., Inc., is now selling its own equipment in the U.S.
Phone: 415/887-3836

EUROPE

Cementation Piling & Foundations, Ltd
Cementation House
Maple Cross, Rickmansworth
Hertfordshire WD3 2SW
ENGLAND

Mr. David Greenwood
Mr. Graham Thomson

Landesgewerbeanstalt Bayern
Gewerbemuseumsplatz 2
8500 Nurnberg 1
W. GERMANY

Dr. Klaus Hilmer

GKN Keller Ltd., U.K. Division
GKN Keller Foundations
Oxford Road, Ryton-on-Dunsmore
Coventry CV8 3EG
ENGLAND

Thorburn and Partners
145 West Regent Street
Glasgow G2 4SA
SCOTLAND

Institut fur Grundbau Bodenmechanik
Paul Gerhardt Allee 2
8 Munchen
W. GERMANY

Building Research Establishment
Garston,
Watford WD2 7JR

Karl Bauer Spezialtiefbau GmbH
Wittelsbacherstrasse 5
8898 Schrobenhausen
W. GERMANY

Vibroflotation (UK) Ltd.
P. O. Box 94
Beaconsfield
Buckinghamshire HP9 1BU
ENGLAND

Franki
196, Rue Gentry
B4020 Liege
Belgique

Dr. J. Michael West
Mr. Klaus Kirsch
Mr. Volker Baumann
Dr. Gerhardt Chambosse
(Munich)
Mr. Heinz Priebe

Mr. Sam Thorburn
Mr. Tom Hindle

Dr. Koreck

Dr. Andrew Charles

Mr. Guenther Oelckers
Fritz Pollens, KG
Halberstadterstr. 6,
1000 Berlin 31, W. Germany

Mr. Peter Thomson

Mr. Maurice Wallays

ASIA
(Sand Compaction Piles)

Dr. Hisao Aboshi
Professor
University of Hiroshima
3-8-2, Sendamachi, Nakaku
Hiroshima, JAPAN

Kensetsu Kikai Chosa Co., Ltd.
8th Floor, Takahashi Minami Bldg.
3-14-16, Nishitenma, Kita-Ku,
Osaka, JAPAN

Mr. Y. Mizutani
Mr. K. Hayashi (USA)

Fudo Construction Co.
4-25, Naka-Ku, Sakee-Cho
Hiroshima, JAPAN 730

Mr. Toyohiko Abe

Nippon Kokan KK
Tsurumi Works
No. 1, 2-Chome, Suehiro-Cho
Tsurumi-Ku, Yokohama,
JAPAN T230

Mr. Miura Yuhichi
Mr. Masatoshi Shimizu

MAA Group
11th Floor
75 Naking East Rd., Sec. 4
Taipai, Taiwan, R.O.C.

Dr. Za-Chieh Moh

Dubon Project Engineering Pvt., LTD.
2, Rehem Mansion, 1st Fl., 44,
S. Bhagat Singh Rd.
Bombay, INDIA 40039

Mr. K. R. Datye
Mr. Bhide
Mr. S. S. Nagaraju

APPENDIX B

LOCAL BEARING FAILURE OF AN ISOLATED STONE COLUMN

Stone columns are an effective method for resisting rotational shear failures involving soft clays in embankments and slopes [9]. For a conventional slope stability analysis, the resisting shear force F developed by the stone column is determined by multiplying the effective normal force, \bar{W}_N , acting on the shear surface by the tangent of the angle of internal friction of the stone, $\tan\phi_s$. The shear capacity, F , of the stone column can, under unfavorable conditions, be limited by a local bearing failure [129] of the stone column and cohesive soil behind the column as illustrated in Figs. 81 and 82.

Now consider the behavior of an isolated, single stone column surrounded by a cohesive soil. If the shear force in the stone column is sufficiently large compared to the strength of the surrounding cohesive soil, a secondary failure surface can develop in the stone column extending downward from the circular arc failure surface (Fig. 81). The resulting wedge of failed stone is bounded above by the circular arc failure surface. The lower failure surface develops within the stone at an angle resulting in the minimum resistance to sliding as defined by force F . The shear force, F , applied to the top causes the wedge (Fig. 82) to slide downward and laterally in the direction of movement of the unstable soil mass above. Sliding of the wedge of stone is resisted by the frictional resistance of the stone developed along the bottom of the wedge and the passive lateral resistance of the adjacent clay. If the passive resistance of the clay is not sufficient, the stone wedge undergoes a local bearing failure by punching into the clay. If a local bearing failure of the clay occurs behind the stone column, the capacity of the column is limited by the secondary wedge failure. A local bearing failure of the clay behind the stone column has been observed by Goughnour [129] during a direct shear test performed in the field on a stone column. Reduced strength of the composite mass was also indicated at Santa Barbara [30] and Steel Bayou [111].

Local Bearing Failure

The limiting shear force that can be applied if a bearing failure controls can be obtained for an isolated column by considering the equilibrium of the wedge shown in Fig. 81. This wedge together with the forces acting on it are illustrated in Fig. 82. The notation shown in this figure is used in the subsequent derivations and is as follows:

- W_s = effective force of stone in the wedge
- $\bar{\gamma}_s$ = effective (bouyant) unit weight of stone in wedge

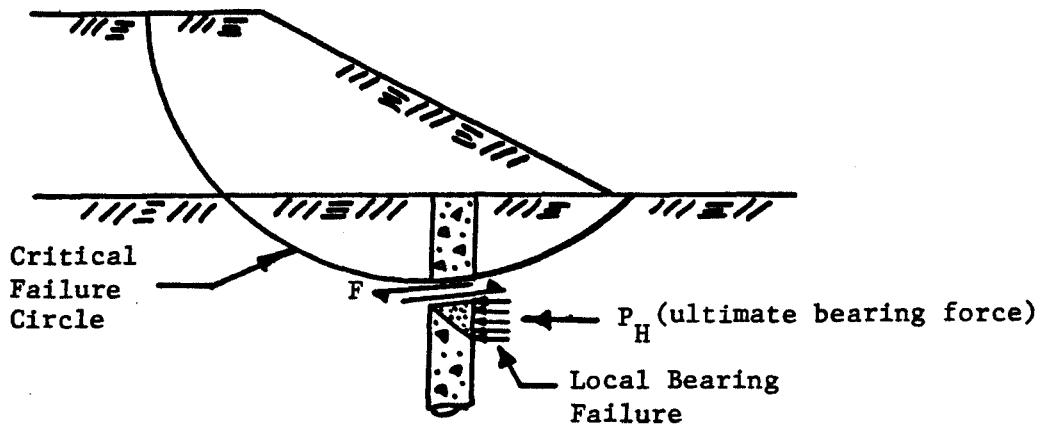


FIGURE 81. WEDGE TYPE LOCAL BEARING FAILURE OF A STONE COLUMN.

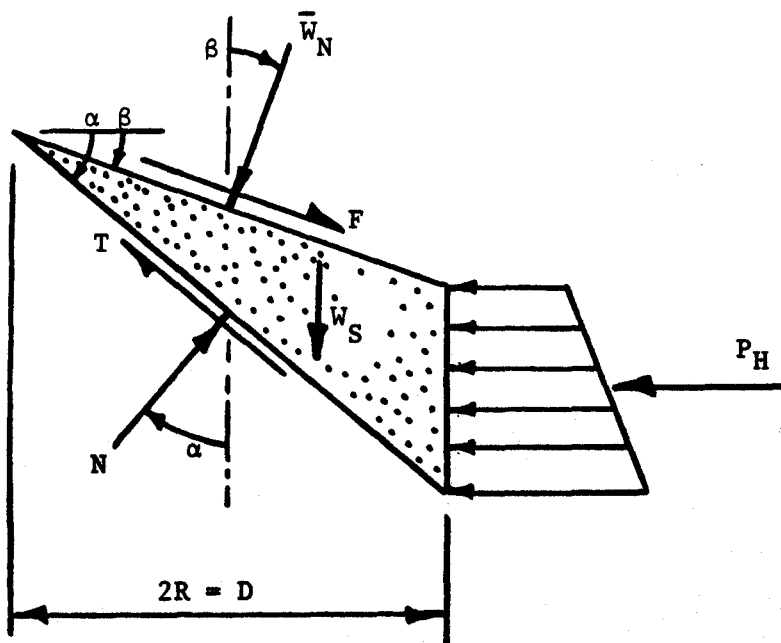


FIGURE 82. LOCAL BEARING CAPACITY FAILURE WEDGE IN STONE COLUMN.

P_H = ultimate lateral resistance of the clay acting on the wedge
 N, T = normal and shear force, respectively, exerted on the bottom surface of the wedge
 \bar{W}_N, F = normal and shear force, respectively, exerted on the top surface of the wedge
 R = radius of the stone column
 D = diameter of the stone column
 ϕ_s = angle of internal friction of the stone
 α, β = angle of inclinations of the lower and upper surfaces of the wedge, respectively.

The upper surface of the wedge makes an angle β with the horizontal. (1)
 This upper surface coincides with the circular arc failure surface (Fig. 81).
 The lower surface of the wedge makes an angle of α with the horizontal. Now
 consider equilibrium of the wedge. To develop the required relationship for
 F , first sum forces acting on the wedge in the vertical direction and solve
 for the unknown normal force N acting on the bottom of the wedge obtaining

$$N = \frac{W_s + \bar{W}_N \cos\beta + F \sin\beta}{\cos\alpha + \tan\phi_s \sin\alpha} \quad (53)$$

where the forces and angles are shown in Fig. 82.

Now sum the forces acting on the wedge in the horizontal direction, substitute for the unknown force N using equation (53), and solve for the limiting force F obtaining

$$F = \frac{\bar{W}_N (\sin\beta + \lambda \cos\beta) + \lambda W_s + P_H}{\cos\beta - \lambda \sin\beta} \quad (54)$$

where: $\lambda = \frac{\tan\phi_s \cos\alpha - \sin\alpha}{\cos\alpha + \tan\phi_s \sin\alpha}$

$$W_s = \pi(\tan\alpha - \tan\beta)R^3\gamma_s$$

In the derivation of equation (54), the effects of adjacent stone columns and outward, lateral spreading of the stone columns were neglected. Neglecting the effect of adjacent columns should introduce a factor of conservatism in predicting the effect of a local bearing failure [130-132]. These effects are offset by neglecting lateral spreading which should be on the unconservative side.

1. R. R. Goughnour of the Vibroflotation Foundation Company has previously developed a solution similar in concept for the special case of $\beta = 0$. His solution handled lateral pressure on the column slightly differently than this solution.

Lateral Bearing Failure in Cohesive Soil

The ultimate passive pressure developed by the cohesive soil as the wedge pushes against it can be calculated using the theory presented by Broms [130] for a single, laterally loaded pile embedded in a frictionless soil. As shown in Fig. 83, the ultimate lateral pressure q_h at the surface is taken to be $q_h = 2c$ with the resistance increasing linearly over a depth of 3 pile diameters where it reaches a maximum limiting value of $q_h = 9c$. The total depth beneath the surface $h + z_0$ (Fig. 84) is considered in determining the 3 pile diameters. Near the surface, the failure occurs due to the upward flow of cohesive soil toward the surface. With increasing depth the failure becomes one of the plastic flow of the soil from the front of the pile around the sides (Fig. 83).

For a single, rough pile having full cohesion, plastic theory [130,131] indicates below a depth of approximately 3 diameters the ultimate lateral capacity is about $q_h = 11$ to $12c$. Use of an ultimate resistance of $9c$, however, is felt to be prudent although it may be slightly on the conservative side. Further, the use of $q_h = 9c$ is reasonable since it is equal to the end bearing capacity of deep piles embedded in a cohesive soil. The value of $q_h = 2c$ used at the surface is also realistic since it equals about 40 percent of the bearing capacity of the clay in the vertical direction.

Now consider the ultimate lateral pressure developed on a wedge of stone making an angle α and β with the horizontal as shown in Fig. 82. Using the pressure distribution shown in Fig. 83, the ultimate passive pressure developed in the clay for a depth $(h + z_0) \leq 3D$ as illustrated in Fig. 84 is

$$P_H = \frac{14}{3} R c \psi [h + z_0 + R(1.714 + \tan\alpha)] \quad (55)$$

and for a depth $h + z_0 > 3D$:

$$P_H = 36R^2 c \psi \quad (56)$$

where: R = radius of stone column
 c = cohesion
 $\psi = \tan\alpha - \tan\beta$
 h = depth of fill above the stone column
 z_0 = depth of the circular arc failure surface below the top of the stone

The sign convention used for α and β is shown in Fig. 84. Once a trial circular arc failure surface has been selected, the value of β is known. The angle α is then determined to give the minimum value of shear force F that can be applied to the top of the wedge before a bearing failure occurs.

Calculation of Limiting Shear Force

The limiting shear force F in each column for a given circular arc sliding surface is calculated as follows:

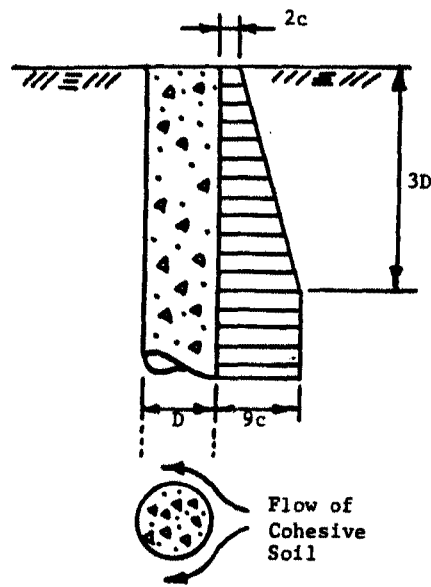


FIGURE 83. BEARING CAPACITY OF A RIGID PILE TRANSLATING Laterally IN A COHESIVE SOIL.

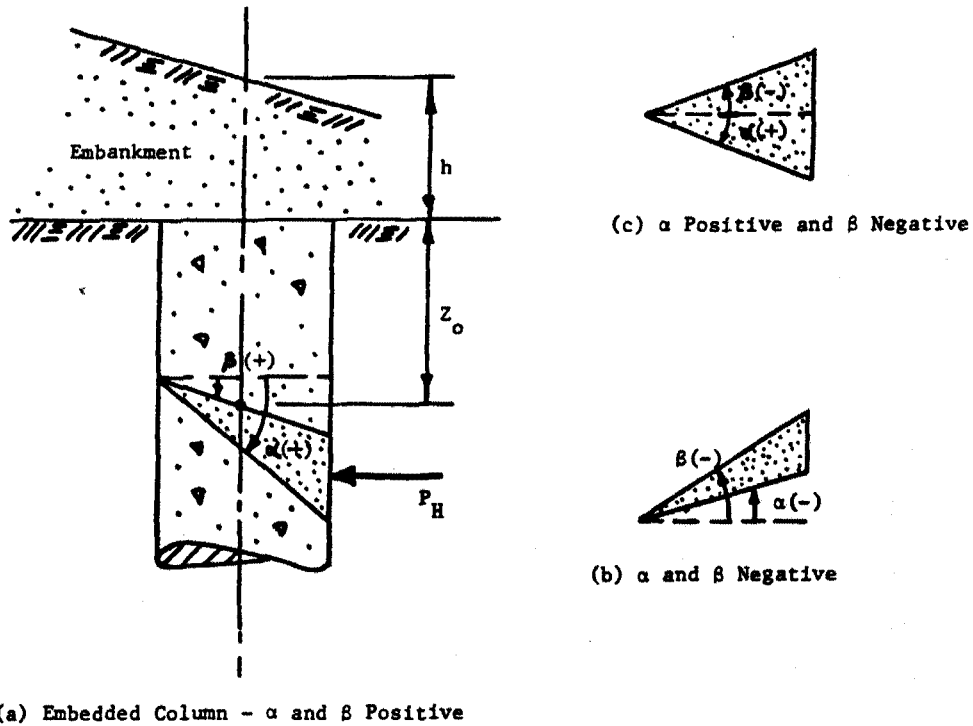


FIGURE 84. NOTATION USED IN FORMULAS FOR LOCAL BEARING FAILURE OF A STONE COLUMN.

1. Determine the angle β for a critical circle and calculate the effective normal force, \bar{W}_N (Fig. 84) at the point on the stone column where the circular arc intersects the center of the stone column (Fig. 81).
2. Select at least three trial values of the angle of inclination α of the lower surface of the wedge.
3. For each value of α calculate the ultimate lateral soil resistance, P_H using equation (55) or (56) and a representative value of the undrained shear strength c of the cohesive soil.
4. For each value of α , calculate F for a bearing failure in the cohesive soil using equation (54).
5. Plot the shear force F obtained from equation (54) as a function of α and select the minimum value of F .
6. Calculate the shear force F that can act on the column if a local bearing failure does not develop: $F = \bar{W}_N \tan \phi_s$.
7. If a local bearing failure of the clay controls the force calculated in Step 5 will be less than that calculated in Step 6. In the stability analysis use the smaller of these forces (or reduce the value of ϕ_s used in design).
8. Repeat the analysis for several selected points along the failure surface.

Design Charts

Figures 85 through 95 present graphically the solution for local bearing failure of a single, isolated stone column for selected design parameters. The procedure for using the charts is as follows:

1. Select tentative design parameters and perform a stability analysis for the stone column improved ground. Plot the critical circle through the stone columns. Examine for the possibility of local failure several points along the critical circle where it intersects the center of the columns. Measure the inclination β of the circle (with the correct sign), and the depth $h + z_0$ of each point (Fig. 84).
2. Calculate the effective vertical force \bar{W}_v acting on the stone column at the depth under consideration by multiplying the vertical effective stress times the area of the stone column. First calculate the effective body stress due to the stone column at the selected point. Use the bouyant unit weight of the stone below the groundwater table. Then calculate the vertical stress σ due to the embankment above the stone column and obtain the stress concentration in the column using $\sigma_s = \mu_s \sigma$ (equation 8b). Add the body stress to σ_s and multiply by the area of the stone column to obtain the effective vertical force \bar{W}_v .

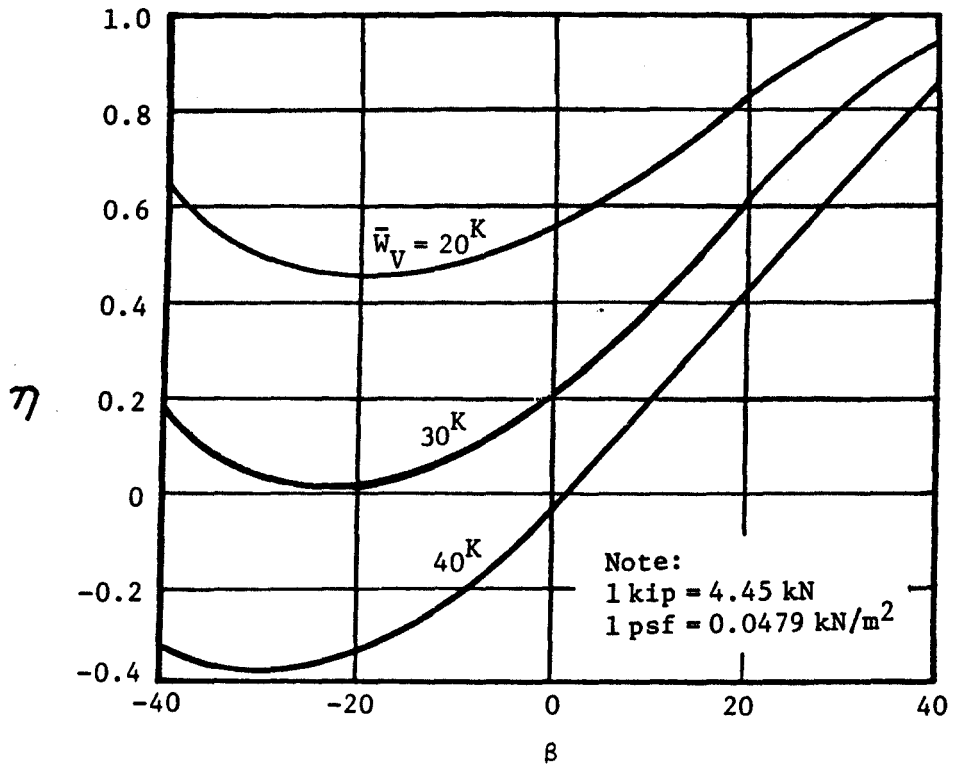


FIGURE 85. LOCAL BEARING FAILURE STABILITY REDUCTION FACTORS FOR DEEP FAILURE: $\phi = 30^\circ$, $c = 100$ PSF.

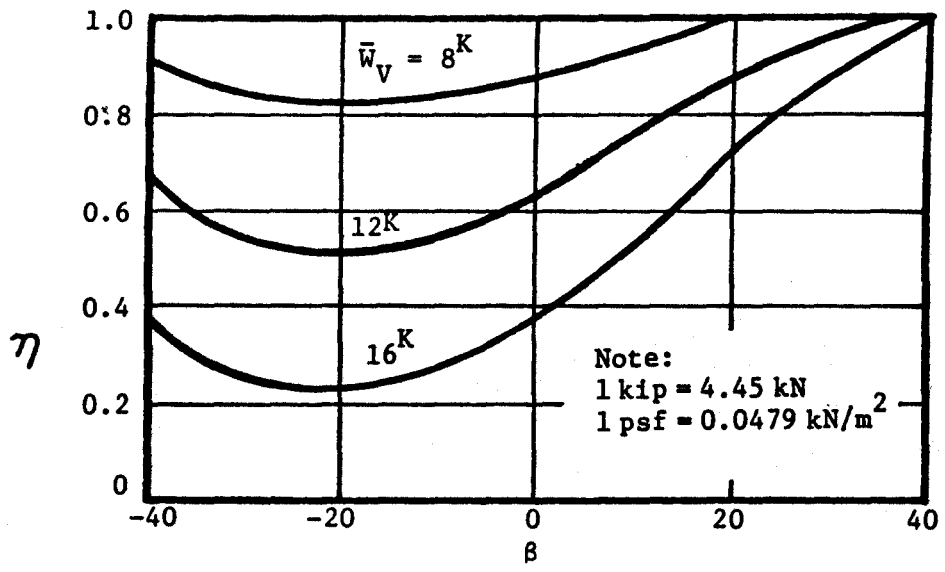


FIGURE 86. LOCAL BEARING FAILURE STABILITY REDUCTION FACTORS FOR SHALLOW FAILURE: $\phi = 30^\circ$, $c = 100$ PSF.

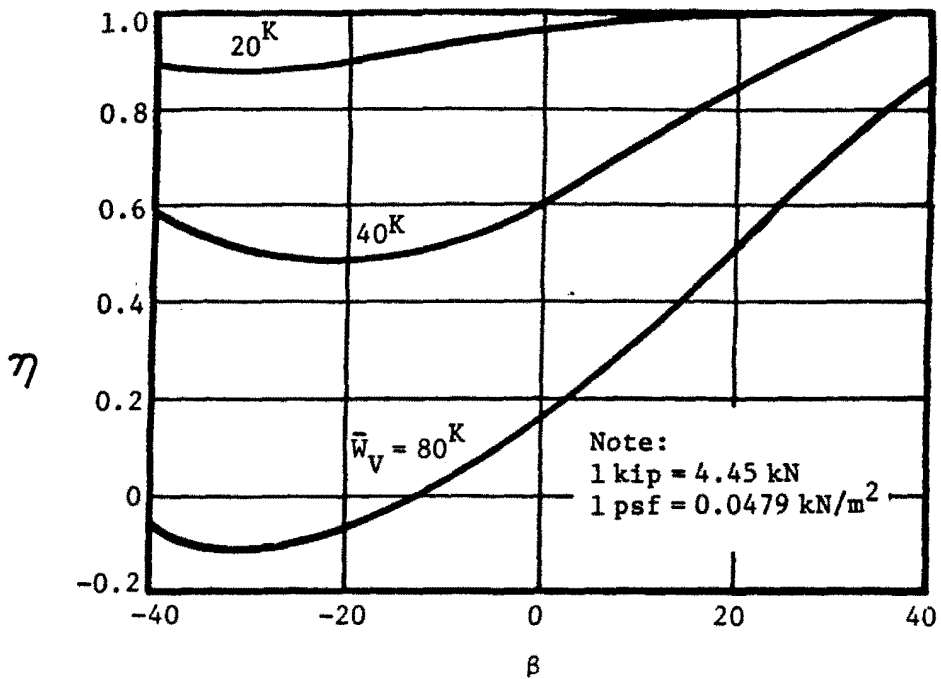


FIGURE 87. LOCAL BEARING FAILURE STABILITY REDUCTION FACTORS FOR DEEP FAILURE: $\phi = 36^\circ$, $c = 200$ PSF.

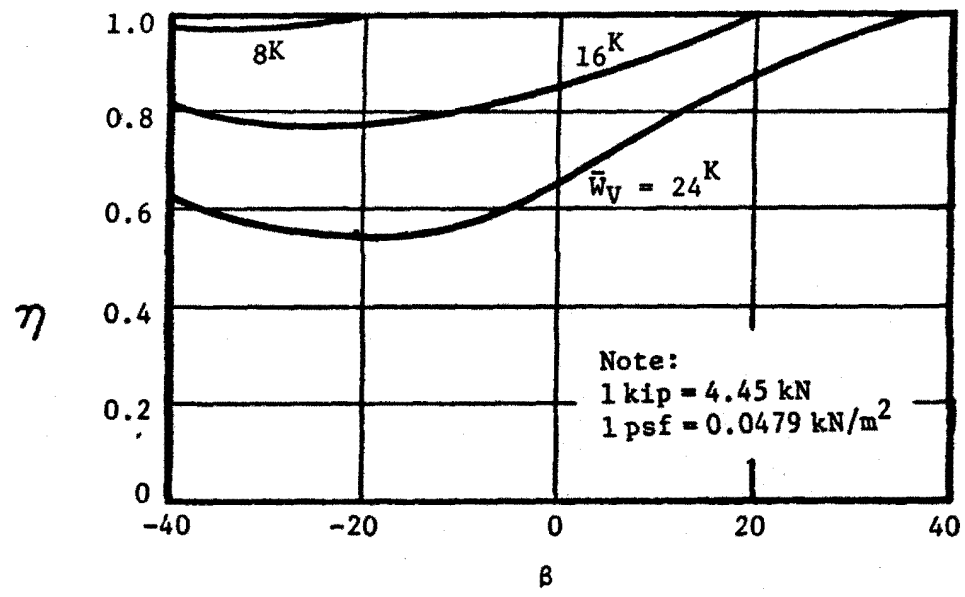


FIGURE 88. LOCAL BEARING FAILURE STABILITY REDUCTION FACTORS FOR SHALLOW FAILURE: $\phi = 36^\circ$, $c = 200$ PSF.

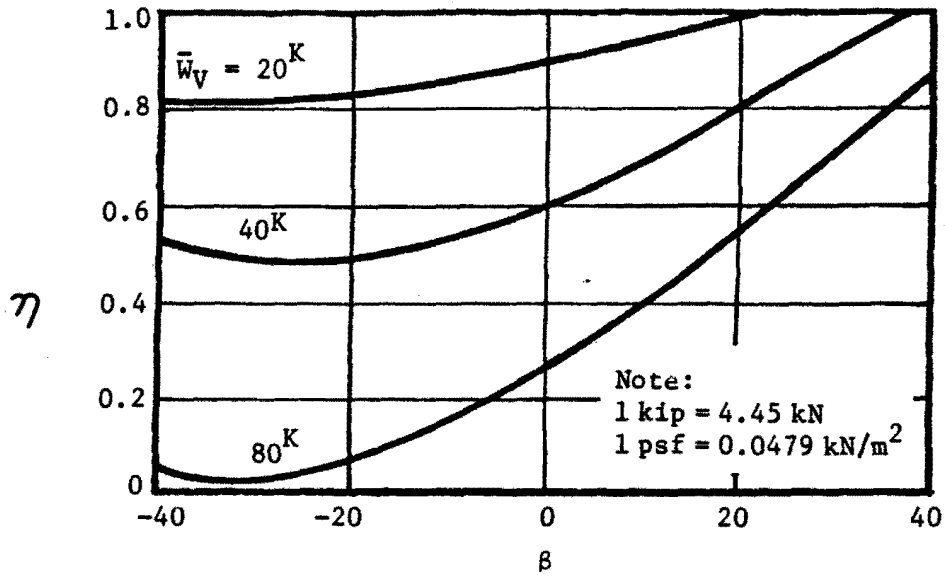


FIGURE 89. LOCAL BEARING FAILURE STABILITY REDUCTION FACTORS FOR DEEP FAILURE: $\phi = 42^\circ$, $c = 200$ PSF.

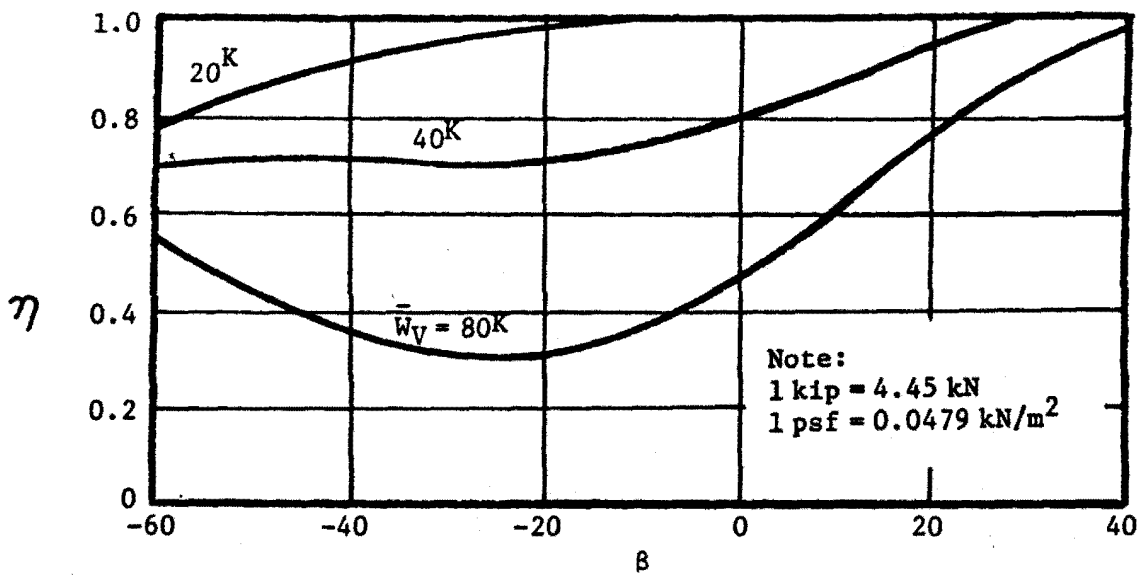


FIGURE 90. LOCAL BEARING FAILURE STABILITY REDUCTION FACTORS FOR DEEP FAILURE: $\phi = 42^\circ$, $c = 300$ PSF.

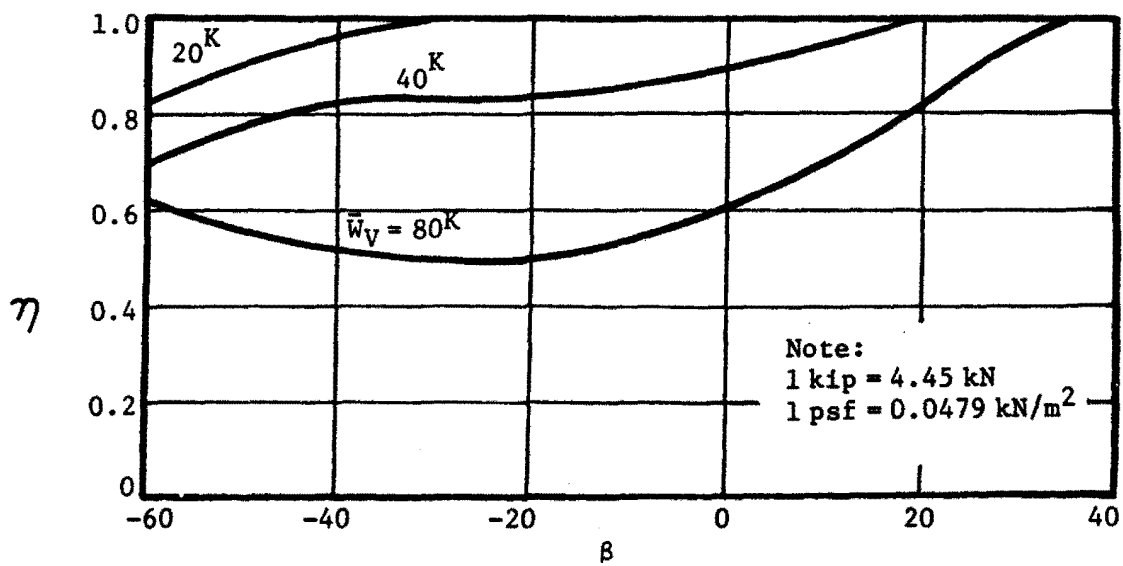


FIGURE 91. LOCAL BEARING FAILURE STABILITY REDUCTION FACTORS FOR DEEP FAILURE: $\phi = 42^\circ$, $c = 400$ PSF.

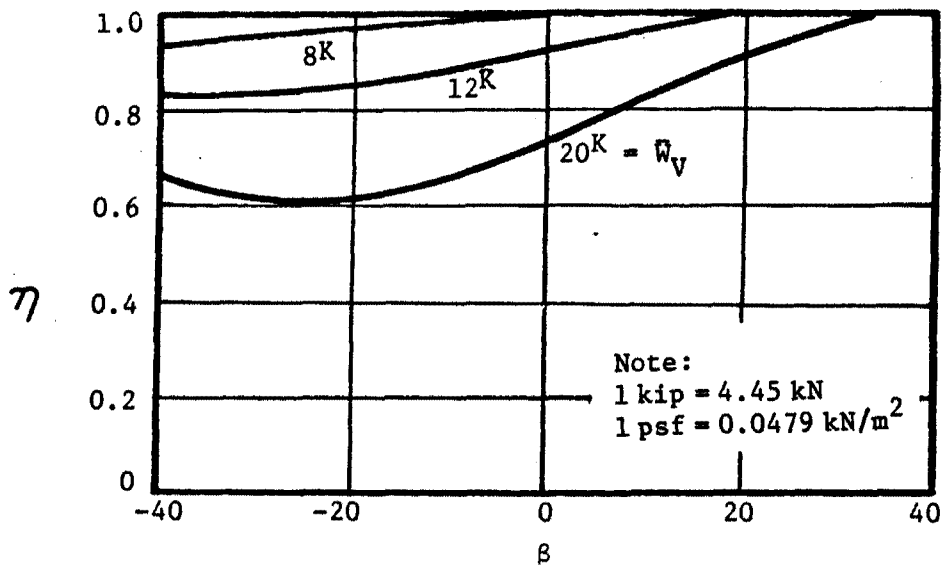


FIGURE 92. LOCAL BEARING FAILURE STABILITY REDUCTION FACTORS FOR SHALLOW FAILURE: $\phi = 42^\circ$, $c = 200$ PSF.

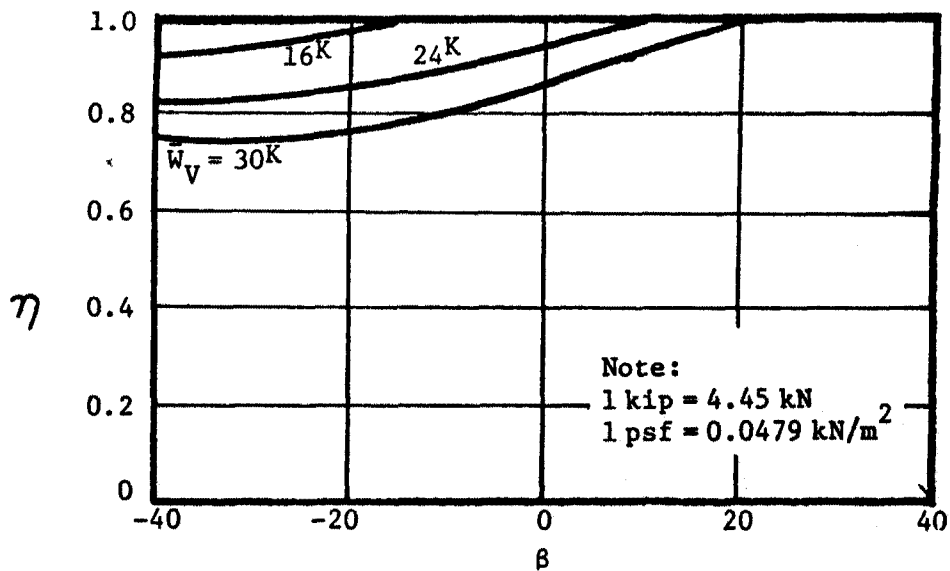


FIGURE 93. LOCAL BEARING FAILURE STABILITY REDUCTION FACTORS FOR SHALLOW FAILURE: $\phi = 42^\circ$, $c = 400$ PSF.

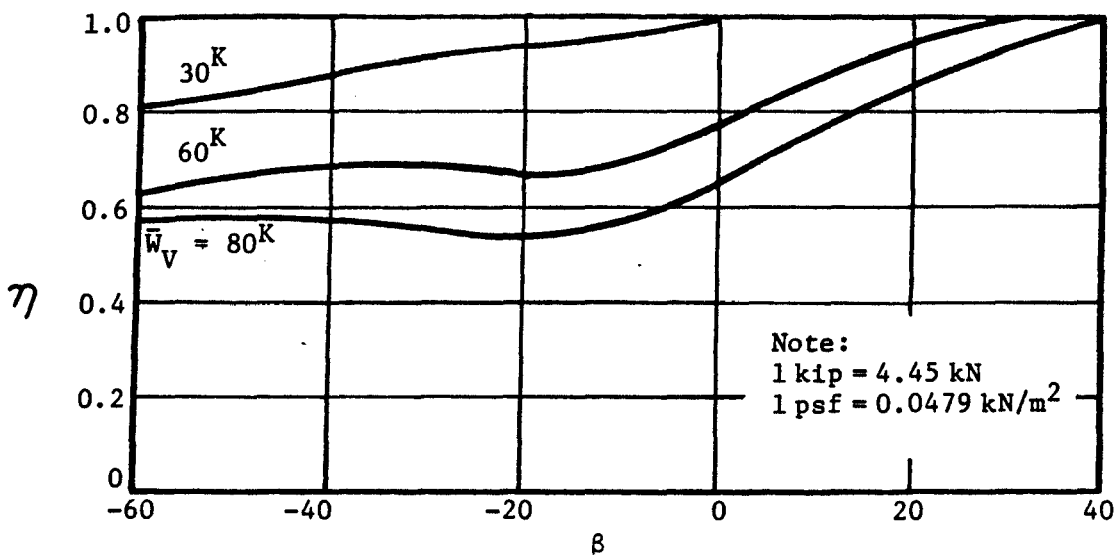


FIGURE 94. LOCAL BEARING FAILURE STABILITY REDUCTION FACTORS FOR DEEP FAILURE: $\phi = 45^\circ$, $c = 600$ PSF.

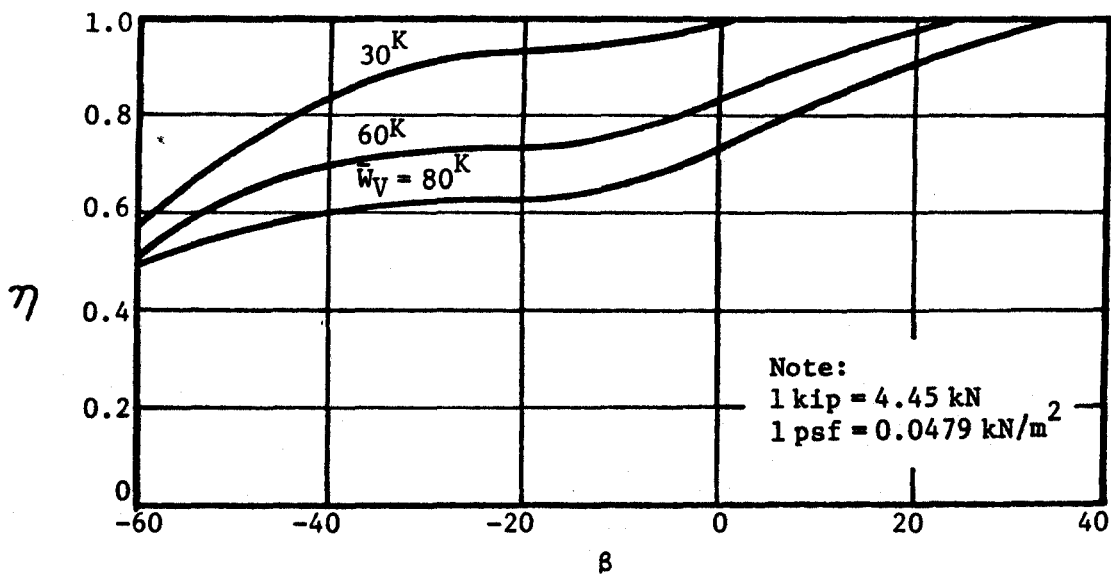


FIGURE 95. LOCAL BEARING FAILURE STABILITY REDUCTION FACTORS FOR DEEP FAILURE: $\phi = 50^\circ$, $c = 800$ PSF.

3. Using \bar{W}_v from Step 2 and the design value(s) of ϕ_s and the cohesion of the clay c , enter the appropriate figure and estimate the value of the reduction factor η .
4. The "deep" charts should be used when the combined embankment height and stone column depth $h + z_o$ is equal to or greater than 3 stone column diameters; otherwise the "shallow" charts should be used.

The ratio η , obtained from these figures, is defined as follows:

$$\eta = \frac{F(\text{from equation 52})}{\bar{W}_N \tan \phi_s}$$

Physically η is the ratio of resisting force that is developed by an isolated stone column if a local bearing failure occurs to the force developed if local failure does not occur (i.e., the force that conventionally would be used in a stability analysis). Hence, η is the reduction factor indicating when a local bearing failure *may* become a problem for the given geometry and material properties used in the design. Theoretically, when $\eta < 1$ local bearing controls the maximum resisting force and moment that can be developed by the stone column. A reduction in resisting force (and moment) developed by the stone column would result in a reduction in safety factor of the slope compared to that computed for a general shear failure.

Design

Full-scale and model direct shear tests indicate a local bearing failure of at least a single stone column is possible. The analysis including the design curves just presented is for a single, isolated stone column. The relatively close proximity of adjacent stone columns and lateral spreading greatly complicate the actual problem compared with an isolated column; certainly further field and model tests are needed in addition to more refined theories. Nevertheless, the design charts and theory presented can be used to indicate when local bearing failure may be a problem. Further, the proposed approach is useful as a general guide in design for selecting safe design parameters (ϕ_s , η).

The likelihood of a local bearing failure increases as the shear strength of the clay decreases, and as a greater angle of internal friction ϕ_s and stress concentration factor η is used in design. For example, if an angle of internal friction, ϕ_s of the stone column of 42° is used, a local bearing *might* occur in cohesive soils having undrained shear strengths less than about 400 psf (19 kN/m²) -- examine Figs. 89 through 93 for typical values of β and \bar{W}_v . A local bearing failure could occur in higher strength cohesive soils if ϕ_s values greater than 42° are used in design. Therefore, when stability is being analyzed in very soft and soft cohesive soils, the effect of a local bearing failure on the overall slope stability should be considered. Also, in firm and stiff soils such an analysis may show use of higher values of ϕ_s may be possible without undergoing a local bearing failure.

Local bearing failure can be easily handled in a slope stability analysis using the concept of a limiting angle of internal friction ϕ_s of the stone. Using this simplified approach several representative points are selected along the critical failure circle(s) as determined by a stability analysis on the stone column improved ground. The effective vertical stress, \bar{W}_v and inclination of the failure circle β (with correct sign) at the selected points is determined. Figs. 85 through 95 can then be used to determine if a local bearing failure might occur at the selected points (and the actual magnitude of the reduction in the resisting shear force F). If a local failure is found not to occur over a significant portion of the failure surface, the design is satisfactory; otherwise consideration should be given to reducing ϕ_s . Note that the figures indicate local failure in general may be a problem only when $\beta < 0$ (i.e., near and to the outside of the toe of the slope). Also, and perhaps more importantly, the charts serve to indicate when local failure is not of concern. In any case past experience and good engineering judgement should be taken into consideration in estimating the stability of the slope.

APPENDIX C
EXAMPLE BEARING CAPACITY PROBLEMS

Bearing Capacity Example 1

Example 1 illustrates prediction of the load due to a wide fill that can be supported by stone column improved ground to avoid a shear failure of the stone columns. The specific problem is to determine what height of fill the stone column improved ground can safely support. Both a general shear failure and a local bulging failure in a deep, very soft clay layer (Fig. 96) must be considered. The subsurface conditions and pertinent parameters needed to solve the problems are shown on Fig. 96. Assume the stone column has an angle of internal friction ϕ_s of 42° , and an equilateral triangular pattern of columns is used having a spacing $s = 7$ ft. (2.1 m)

1. Calculate the area replacement ratio a_s from equation 5b:

$$a_s = 0.907 \left(\frac{D}{s}\right)^2 = 0.907 \left(\frac{3.5 \text{ ft.}}{7 \text{ ft.}}\right)^2 = 0.227 \quad (5b)*$$

$$A_s = \pi \cdot D^2 / 4 = 3.14(3.5 \text{ ft.})^2 / 4 = 9.62 \text{ ft.}^2$$

$$A = A_s / a_s = 9.62 \text{ ft.}^2 / 0.227 = 42.4 \text{ ft.}^2 \text{ (total area)} \quad (3)*$$

Note that all numbers in parentheses with an asterisk given to the side of an equation used in the example problems refer to equations given in the main text.

2. Stone Column. Estimate the general ultimate capacity of the stone column using equation (50) assuming a bulging failure occurs in the upper three stone column diameters of depth. Since the clay has a $\tilde{a}PI < 30$ and is not classified as very soft ($c < 250$ psf), use $\tilde{N}_c = 22$ (refer to Chapter VII).

$$\tilde{q}_{ult} = c\tilde{N}_c = 0.45 \text{ ksf} (22) = 9.9 \text{ ksf} \quad (50)*$$

$$P_{ult} = \tilde{q}_{ult} A_s = 9.9 \text{ ksf} (9.62 \text{ ft.}^2) = 95.2 \text{ k}$$

In the above expressions the stress in the stone column at ultimate is $\sigma_s = \tilde{q}_{ult} = c\tilde{N}_c$.

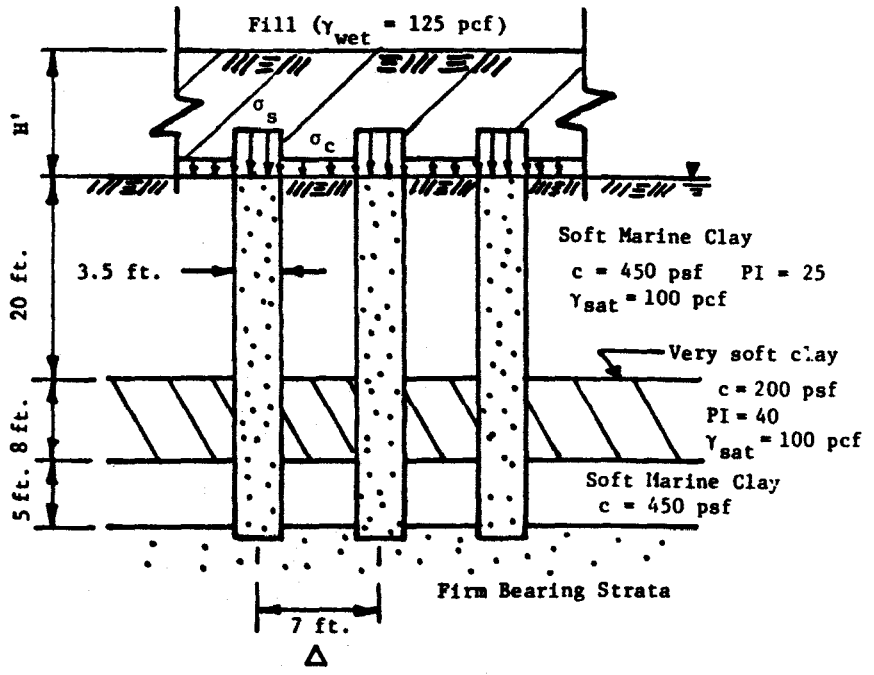


FIGURE 96. BEARING CAPACITY EXAMPLE 1 - WIDE FILL OVER STONE COLUMN IMPROVED CLAY.

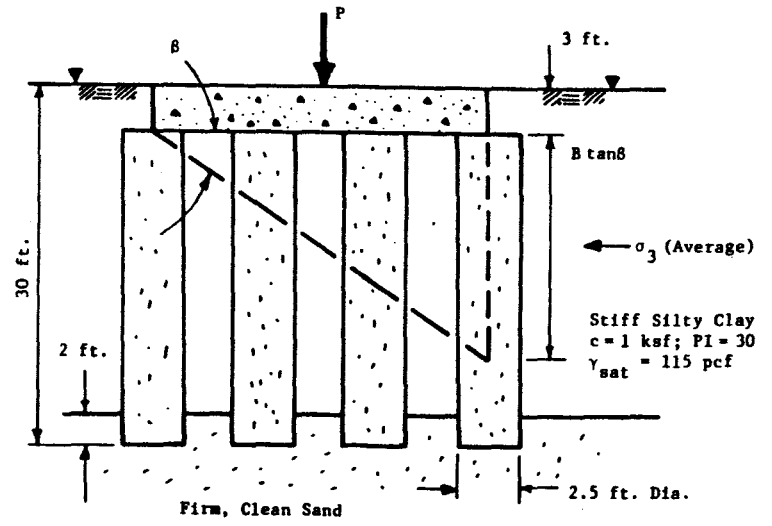
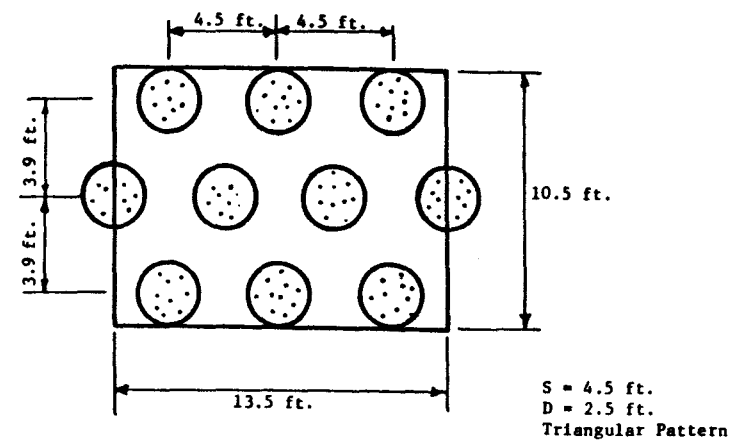


FIGURE 97. BEARING CAPACITY EXAMPLE 2.

3. Deep Bulging. Now check for the possibility of a bulging failure in the very soft clay stratum located at a depth of 20 ft. As discussed in Appendix B the ultimate lateral stress which an isolated stone column can develop is approximately equal to $\sigma_3 \approx 9c = 9(0.2 \text{ ksf}) = 1.8 \text{ ksf}$ since the weak stratum is greater than $3D$ below the surface. From equation (9) the ultimate stress the stone column can carry is then

$$\bar{q}_{ult} = \sigma_3 (1 + \sin\phi_s) / (1 - \sin\phi_s) = 1.8 \text{ ksf} \quad (9)^*$$

$$\bar{q}_{ult} = 9.07 \text{ ksf}$$

Since the ultimate stress the stone column can carry considering a deep bulging failure in the very soft layer is slightly less than for a failure at the surface, the very soft deep stratum controls.

4. Cohesive Soil. The maximum ultimate stress the clay surrounding the stone column can take is $\sigma_c = 5c = 5(0.450 \text{ ksf}) = 2.25 \text{ ksf}$. However, the total load applied to the unit cell must also not overload the clay. Assuming an $n=3$, from equations (8a) and (8b)

$$\mu_s = n / [1 + (n-1) a_s] = 3 / [1 + (3-1) 0.227] = 2.06$$

$$\mu_c = 1 / [1 + (n-1) a_s] = 1 / [1 + (3-1) 0.227] = 0.688$$

$$\text{Then } \sigma_c \leq \mu_c \sigma = \mu_c (\sigma_s / \mu_s)$$

$$\sigma_c < \mu_c \sigma = 0.688 (9.07 \text{ ksf}) / 2.06 = 3.0 \text{ ksf}$$

Since 3.0 ksf is greater than $5c = 2.25 \text{ ksf}$, $\sigma_c = 5c = 2.25 \text{ ksf}$ is the ultimate stress the clay can carry.

5. Allowable Fill Loading. The ultimate loading that can be applied over the unit cell area well within the fill area is

$$P_{ult} = \sigma_s A_s + \sigma_c A_c = (9.07 \text{ ksf})(9.62 \text{ ft.}^2) + (2.25 \text{ ksf})(32.8 \text{ ft.}^2)$$

$$P_{ult} = 161 \text{ k}$$

Using a safety factor of 2.0 the allowable loading is $P_{all} = 161 \text{ k} / 2 = 80.5 \text{ k}$. The height of embankment that will apply the safe loading to the unit cell is $\gamma_{wet}^{fill} H' = \sigma = P_{all} / A$.

Hence

$$H' = P_{\text{all}} / (\gamma_{\text{wet}}^{\text{fill}} \cdot A) = 80.5 \text{ k} / (0.125 \text{ kcf} \times 42.4 \text{ ft.}^2)$$

$$H' = 15.1 \text{ ft.}$$

6. Commentary. Settlement of the fill would be significant and should be calculated. Also, the stability at the edge of the fill should be checked using a circular arc analysis. In this example the very soft clay layer at a depth of 20 ft. controls the load that can be applied to the stone columns. Use of an ultimate lateral stress of $9c$ acting on the stone columns should give a conservative, but realistic, estimate of the ultimate resistance to bulging that can be developed (refer to Appendix B for a more indepth consideration of this aspect).

Using $\sigma_3 = 9c$ as the limiting lateral pressure the soil can withstand, the ultimate load a stone column can carry would for $\phi_s = 42^\circ$ be equal for depths greater than $3D$ to $\bar{q}_{\text{ult}} = 9c (1 + \sin\phi_s) / (1 - \sin\phi_s) = 9c (5.04) = 45c$ or $\bar{N}_c = 45$ which indicates a limiting value of \bar{N}_c exists at a deep depth.

Because the fill is wide, the stress on the stone column does not decrease with depth due to lateral spreading of stress. If a narrow group of stone columns had been used, the stress would, however, decrease with depth; this could be taken into account to determine the increased stress that could be applied at the surface compared with the level of the very soft clay stratum which controlled.

Finally, Vesic cavity expansion theory could also have been used to determine the ultimate capacity of the stone column in the weak stratum. Since the clay is very soft and has a $PI > 30$, $E = 5c$ is used to calculate a Rigidity Index, I_r (equation 13) of 1.72 for $\nu_s = 0.45$. In this analysis let q = the total lateral stress acting at the center of the soft layer. Nonlinear finite element analyses indicate the lateral pressure due to the applied surface loading σ_c can be conservatively approximated as $0.4\sigma_c$:

$$q = K_o \gamma z + 0.4\sigma_c = 0.75(24 \text{ ft.})(0.1 \text{ kcf}) + 0.4(2.25 \text{ ksf})$$

$$q = 2.7 \text{ ksf}$$

Now $F'_c = \ln I_r + 1 = \ln 1.72 + 1 = 1.54$ for $\phi_c = 0$ and no volume change. Then the ultimate load the stone column can carry is

$$q_{\text{ult}} = [c F'_c + q F'_q] (1 + \sin\phi_s) / (1 - \sin\phi_s) \tag{14}^*$$

$$q_{\text{ult}} = [0.2 \text{ ksf} (1.54) + 2.7 \text{ ksf} (1)] [5.04] = 15.1 \text{ ksf}$$

Because of the large effect of overburden pressure, cavity expansion theory appears to overestimate the load which the stone column can carry through the very soft clay stratum.

Bearing Capacity Example 2: Square Group

Stone columns are to be used to improve a stiff clay to slightly reduce settlement of a foundation 13.5 ft. by 10.5 ft. (4.1 m x 3.2 m) in plan (Fig. 97). The modular ratio between the stone columns and the surrounding clay is estimated to be 6.0. Determine the ultimate and safe bearing capacity of the ten stone column group illustrated in Fig. 97. The material properties and geometries involved are shown on the figure.

From Fig. 27 the stress concentration in the stone column improved ground is about 2.0. The bearing capacity calculations are as follows:

1. Calculate the area replacement ratio, a_s

$$A_s = \frac{3.14}{4} (2.5 \text{ ft.})^2 \times 10 = 49.1 \text{ ft.}^2; \quad A = 13.5 \text{ ft.} \times 10.5 \text{ ft.} = 141.8 \text{ ft.}^2;$$

$$a_s = A_s / A = 49.1 \text{ ft.}^2 / 141.8 \text{ ft.}^2 = 0.346$$

2. Determine the stress concentration in the stone column from equation (8b) (or Fig. 68):

$$\mu_s = n / [1 + (n-1) a_s] = 2 / [1 + (2-1)(0.346)] = 1.49 \quad (8b)^*$$

3. Calculate the composite shear strength within the stone column group (equation 16a and equation 16b) and related parameters.

$$[\tan\phi]_{\text{avg}} = \mu_s \tan\phi_s (a_s) = (1.49) \tan 42.0^\circ (0.346) = 0.464 \quad (16a)^*$$

$$\phi_{\text{avg}} = \tan^{-1} (0.464) = 24.9^\circ$$

$$\tan\beta = 1.566 \quad \tan^2\beta = 2.454$$

$$c_{\text{avg}} = c \times (1 - a_s) = 1 \text{ ksf} (1 - 0.346) = 0.654 \text{ ksf} \quad (16b)^*$$

4. Using Vesic cavity expansion theory, calculate the ultimate lateral stress σ_3 in the clay surrounding the stone column group. Since the clay is stiff, has no organics and has a PI = 30, use $E = 11c$ for calculating the Rigidity Index, I_r . The average diameter of the foundation is $B = \sqrt{4A/3.14} = 13.4 \text{ ft.}$ The depth of the failure wedge is then (Fig. 97) $B \tan\beta + 3 \text{ ft.} = (13.4 \text{ ft.})(1.566) + 3 \text{ ft.} = 24 \text{ ft.}$ The initial lateral stress in the stiff silty clay surrounding the stone columns will be used as a conservative estimate of the mean stress q (equation 12),

for use in the cavity expansion theory. The stiff silty clay is known to be normally consolidated. Therefore from reference 62, p.300, $K_c \approx 0.6$ for the surrounding silty clay, and $q \approx 0.6$ (13.5^o ft. x 0.115 kcf) = 0.931 ksf. Now calculate the Rigidity Index (equation 13):

$$I_r = \frac{E}{2(1+\nu)(c+q \tan \phi)} = \frac{11c}{2(1+0.45)(c+q \tan 0^\circ)} \quad (13)*$$

giving $I_r = 3.79$. From $F'_c = 2 \ln I_r + 1$ for $\phi = 0$ and Fig. 19, $F'_c = 2.33$ and $F'_q = 1.0$. Then calculate the ultimate lateral stress which can be developed by the surrounding silty clay:

$$\sigma_3 = c F'_c + q F'_q = 1 \text{ ksf} (2.33) + 0.931 \text{ ksf} (1.0) = 3.26 \text{ ksf} \quad (12)*$$

5. Calculate the ultimate vertical stress and load that can be applied over the rigid foundation (see equation 19 in text):

$$q_{ult} = \sigma_1 = \sigma_3 \tan^2 \beta + 2c_{avg} \tan \beta = 3.26 \text{ ksf} (2.454) + 2(0.654 \text{ ksf})$$

$$(1.566)$$

$$(19)*$$

$$q_{ult} = 8.0 \text{ ksf} + 2.0 \text{ ksf} = 10.0 \text{ ksf}$$

The ultimate load that can be carried by the foundation is $P_{ult} = q_{ult} \cdot A = 10.0 \text{ ksf} (141.8 \text{ ft.}^2) = 1418 \text{ k}$. Using a safety factor of 2.0, the foundation can carry $P_{ult} = 1418 \text{ k} / 2.0 = 709 \text{ k}$. This amounts to 70.9 k (or 35.5 tons) per stone column if the silty clay is assumed not to carry any of the load. This level of loading is reasonable for a foundation where settlement is of concern (refer to Table 12).

6. Commentary. Settlement of course would control the design. A total load on the group of 709 k would be used for a first settlement estimate. For this loading, the average stress applied to the foundation is $\sigma = 709 \text{ k} / 141.8 \text{ ft.}^2 = 5 \text{ ksf}$. The probable distribution of stress between the stone and soil for $n = 2$ would be

$$\sigma_c = \mu_c \sigma = 0.743 (5 \text{ ksf}) = 3.7 \text{ ksf}$$

$$\sigma_s = \mu_s \sigma = 1.49 (5 \text{ ksf}) = 7.45 \text{ ksf}$$

Since the ultimate stress of the stiff clay is about $6.2c = 6.2 \text{ ksf}$, the stress level in the clay is not excessive. Using the proposed design, the ratio of the settlement of the treated to unimproved

ground would approximately be $S_t/S \approx \mu_c = 0.74$ (refer to equations 20, 21 and 22). Thus for the conditions analyzed, reduction in settlement on the order of 25 percent would be expected. For the given site conditions, use of a larger footing (without stone columns) should also be evaluated considering magnitude of settlements and the economics of the designs.

In general for the wet method a stone column spacing less than 5 ft. is not recommended; Example Problem 2 would therefore be an exception because of the presence of the stiff, silty clay.

APPENDIX D
EXAMPLE SETTLEMENT PROBLEMS

Settlement Example 1

Settlement Example 1 illustrates calculating settlements of a soft clay reinforced with stone columns and loaded by a wide fill. The calculation of the load carrying capacity of stone column improved ground for a problem similar to this was illustrated by Example 1 in Appendix C. In the present example, primary consolidation settlements are calculated using both the equilibrium and finite element methods. Secondary settlements are also calculated. The problem is illustrated in Fig. 98. The site consists of 20 ft. (6.1 m) of gray, soft silty clay overlying a firm to dense sand. The groundwater table is at the surface. An equilateral triangular pattern of stone columns is used having a spacing of 6.5 ft. (2 m). The diameter of the stone column is estimated (Table 13) to be 3.5 ft. (1.07 m). A 2.5 ft. (0.7 m) sand blanket is to be placed over the soft silty clay for a working platform and drainage blanket.

Equilibrium Method. The average stress σ exerted by the 2.5 ft. sand blanket and 12.5 ft. structural fill on the top of the stone columns is $\sigma = 12.5 \text{ ft.} \times 120 \text{ pcf} + 2.5 \text{ ft.} (108 \text{ pcf}) = 1770 \text{ psf}$. The area replacement ratio, a_s from equation (5b) is for an equilateral, triangular stone column pattern

$$a_s = 0.907 (D/s)^2 = 0.907 \left(\frac{3.5 \text{ ft.}}{6.5 \text{ ft.}}\right)^2 = 0.263 \quad (56)*$$

Assume for the *settlement analysis* the stress concentration factor n to be 5.0. Then the stress concentration factor μ_c in the clay is from equation (8a) or Fig. 68

$$\mu_c = 1/[1 + (n - 1) a_s] = 0.487 \quad (8a)*$$

The initial effective stress $\bar{\sigma}_0$ at the center of the silty clay layer is

$$\bar{\sigma}_0 = 10 \text{ ft.} \times (95 \text{ pcf} - 62.4 \text{ pcf}) = 326 \text{ psf}$$

* These numbers refer to equations previously given in the main text.

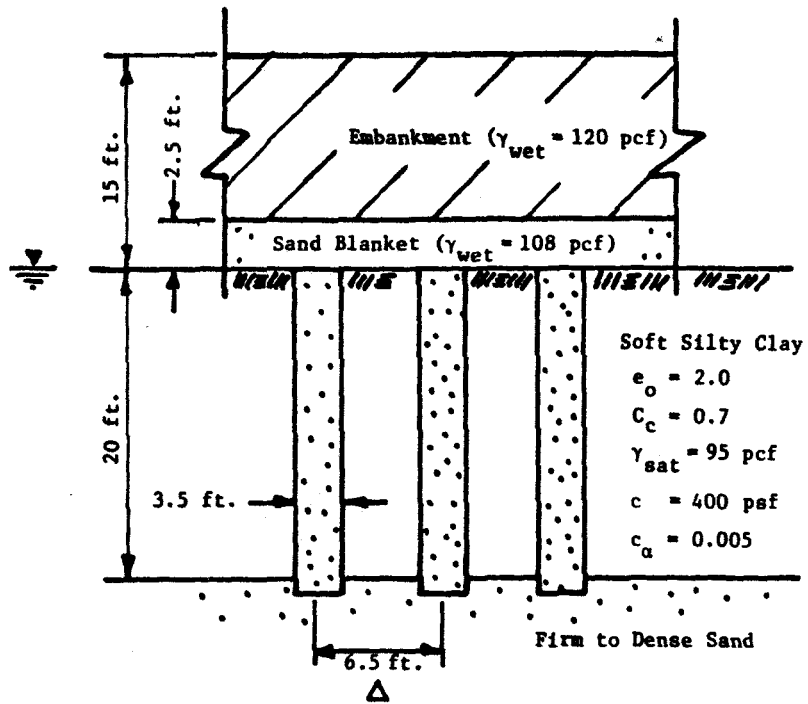


FIGURE 98. SETTLEMENT EXAMPLE 1 - WIDE FILL OVER STONE COLUMN IMPROVED SILTY CLAY.

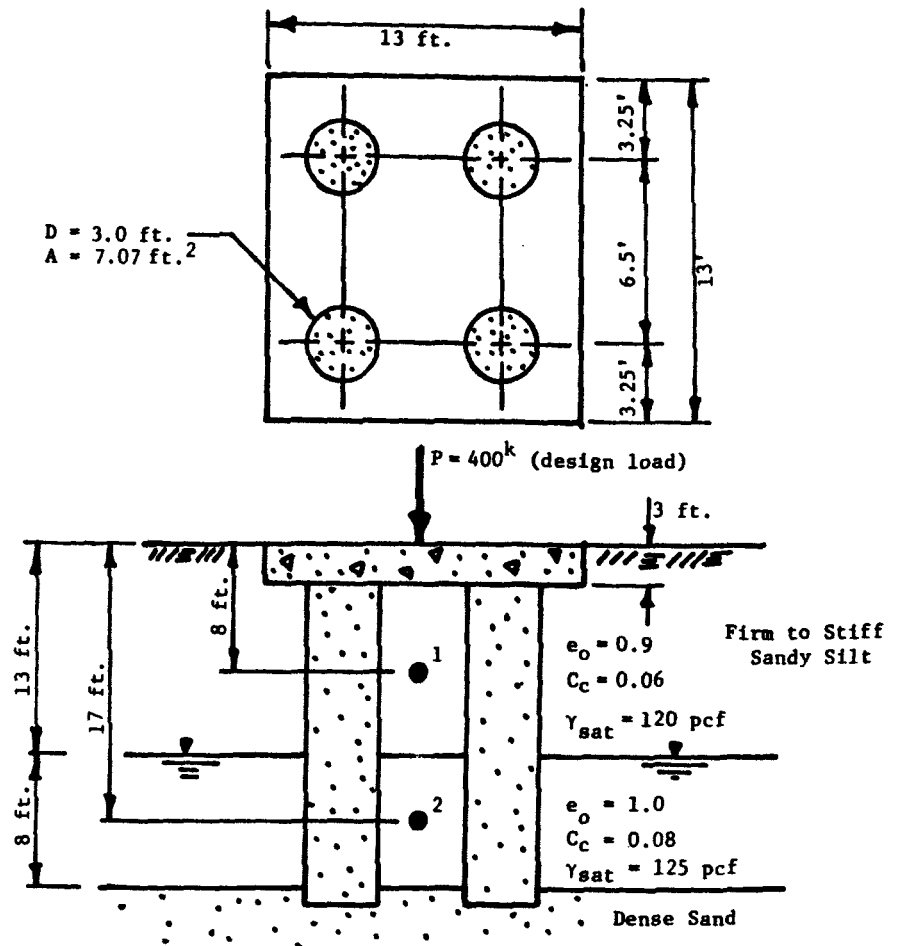


FIGURE 99. SETTLEMENT EXAMPLE 2 - RIGID FOUNDATION PLACED OVER STONE COLUMN IMPROVED SANDY SILT.

The primary consolidation settlement in the clay layer from one-dimensional consolidation theory is from equation (20)

$$S_t = \frac{C_c}{1+e_o} \log_{10} \left(\frac{\bar{\sigma}_o + \sigma_c}{\bar{\sigma}_o} \right) \cdot H \quad (20)*$$

$$S_t = \left(\frac{0.7}{1+2.0} \right) \log_{10} \left(\frac{326 \text{ psf} + (1770 \text{ psf})(0.487)}{326 \text{ psf}} \right) \cdot (20 \text{ ft.} \times 12 \text{ in./ft.})$$

$$S_t = 31.4 \text{ in.}$$

The estimated primary consolidation settlement of the stone column improved silty clay layer is thus 31 in. following the equilibrium method. For comparison, the settlement in the silty clay layer if not improved with stone columns would be 45.2 in.

Note how simple the equilibrium method is to apply to a problem. The "trick", of course, is to estimate the correct value of stress concentration factor n to use in the analysis. In this problem the fill was wide and no dissipation laterally of stress with depth occurs. The next settlement example shows how both the equilibrium and the finite element methods can be applied to a problem where the applied stress decreases with depth.

Nonlinear Finite Element Method. Since the clay is soft and quite compressible use the nonlinear finite element method of analysis. First calculate the modulus of elasticity E_c of the clay for the approximate stress range of interest. The initial average stress in the clay from the equilibrium method is $\bar{\sigma}_o = 326$ psf. The change in stress in the clay due to the embankment loading is $\sigma_c = \mu_c \sigma = 0.559 (1770) \text{ psi} = 989$ psf. Using Table 10 and experience as a guide, the drained Poisson's ratio of the clay is assumed to be 0.42 from equation (47). The modulus of elasticity of the clay for the applicable stress range is

$$E_c = \frac{(1+\nu)(1-2\nu)(1+e_o) \sigma_{va}}{0.435 (1-\nu) C_c} = \frac{(1+0.42)(1-2 \times 0.42)(1+2.0)}{0.435 (1-0.42)(0.70)} \frac{(326 \text{ psf} + 989 \text{ psf})}{2}$$

$$E_c = 2538 \text{ psf} = 17.6 \text{ psi}$$

Note that the value of Poisson's ratio selected has a significant effect on the calculated value of E_c : larger values of ν_c give smaller values of E_c .

The stone column length to diameter ratio in the soft clay is, $L/D = 20 \text{ ft.} / 3.5 \text{ ft.} = 5.7$. The average applied pressure σ due to the embankment is $\sigma = 1770 \text{ psf} = 12.3 \text{ psi}$. Interpolating from Figs. 32 and 33 ($a_g = 0.25$) for a soft boundary condition ($E_b = 12 \text{ psi}$), the effective ratio of settlement of

stone column reinforced ground to stone column length, $S/L = 0.078$. (In interpolating between figures for different S/L values, work in terms of settlement since the length varies). The embankment settlement from the finite element method is then $S = 0.078$ (20 ft. x 12 in./ft.) = 19 in. The "best" settlement estimate is the average of the finite element and incremental methods

$$S_t = (19 \text{ in.} + 31 \text{ in.})/2 = 25 \text{ in.}$$

The estimated reduction in settlement due to stone column improvement is then $S_t/S = 25.0 \text{ in.}/45.2 = 0.586$.

Time Rate of Settlement. Determine the magnitude of primary consolidation settlement after 2 months assuming instantaneous construction⁽¹⁾. The silty clay has a vertical coefficient of consolidation C_v of 0.05 ft.²/day. Based on a detailed study of the strata, the horizontal permeability is estimated to be 3 times the vertical permeability. Then from equation (49)

$$C_{v_r} = C_v (k_h/k_v) = 0.05 \text{ ft.}^2/\text{day} (3) = 0.15 \text{ ft.}^2/\text{day} \quad (49)*$$

Assume the reduced drain diameter D' to account for smear is 1/5 the constructed stone column diameter. For an equilateral triangular stone column spacing s of 6.5 ft., the equivalent diameter D_e of the unit cell is

$$D_e = 1.05s = 1.05 (6.5 \text{ ft.}) = 6.83 \text{ ft.} \quad (1)*$$

and

$$n^* = r_e/r_w = D_e/D' = 6.83 \text{ ft.}/(3.5 \text{ ft.}/5) = 9.76 \quad (\text{Fig. 45})$$

The dimensionless vertical and horizontal time factors are then

$$T_z = C_v t / (H/N)^2 = 0.05 \text{ ft.}^2/\text{day} (2 \times 31 \text{ days}) / (20 \text{ ft.}/2)^2 = 0.031 \quad (27)*$$

$$T_r = C_{v_r} t / (D_e)^2 = 0.15 \text{ ft.}^2/\text{day} (2 \times 31 \text{ days}) / (6.83 \text{ ft.})^2 = 0.199 \quad (28)*$$

From Fig. 42, $U_z = 0.12$ and from Fig. 43, $U_r = 0.64$. The combined degree of consolidation, equation (25), is

1. Methods for handling construction over a finite time interval are given elsewhere [88].

$$U = 1 - (1 - U_z)(1 - U_r) = 1 - (1 - 0.12)(1 - 0.64) = 0.68 \quad (25)*$$

An important portion of the total primary consolidation settlement occurs after 2 months and equals $S'_c = 25.0 \text{ in.}(0.68) = 17 \text{ in.}$ For this example problem having stone columns, vertical drainage had little effect on the time rate of primary settlement, due to the higher radial coefficient of consolidation and smaller radial drainage path to the vertical drains. For comparison, if stone columns had not been used, primary consolidation settlement would have been only 12 percent complete, with the primary settlement at the end of two months being only about 3 in.

Secondary Compression Settlement. Estimate the magnitude of secondary compression settlement that would be expected to occur 5 years after construction. Assume secondary compression begins at the time for 90 percent primary consolidation. Neglect the effects of vertical drainage which were shown above to be small. The radial time factor for 90 percent primary consolidation for $n^* = 9.76$ is $U_r = 0.47$ from Fig. 43. From Equation (28) the time for 90 percent primary consolidation is $t = T_r(D_e)^2/C_{v_r} = 0.47 (6.83 \text{ ft.})^2 / (0.15 \text{ ft.}^2/\text{day}) = 146 \text{ days}$ after construction. The secondary compression settlement is then

$$\Delta S = C_\alpha H \log_{10}(t_2/t_1) \quad (30)*$$

$$\Delta S = 0.005(240 \text{ in.}) \log_{10}(5(365 \text{ days})/146 \text{ days}) = 1.3 \text{ in.}$$

For the silty clay in this problem, the secondary settlement is thus relatively small compared to a primary consolidation settlement of 26.5 in. If organics had been present secondary settlement would have been significantly greater.

Settlement Example 2

Settlement Example 2 illustrates how to handle, at least approximately, stress distribution in calculating settlement of stone column improved ground. Stone column improved ground is being considered as one design alternative for a slightly marginal site consisting of firm to stiff sandy silt as shown in Fig. 99. The average contact stress is $\sigma = P/A = 400 \text{ kips (13 ft. x 13 ft.)} = 2367 \text{ psf}$. The gross area replacement ratio from equation (3) is $a_g = A_g/A = (7.07 \text{ ft}^2)(4)/(13 \text{ ft. x 13 ft.}) = 0.167$. Now determine the initial effective stress at the center of each layer:

$$\text{Layer 1: } \bar{\sigma}_o = 8 \text{ ft. (120 pcf)} = 960 \text{ psf}$$

$$\begin{aligned} \text{Layer 2: } \bar{\sigma}_o &= 13 \text{ ft. (120 pcf)} + 4 \text{ ft. (125 pcf - 62.4 pcf)} \\ &= 1810 \text{ psf} \end{aligned}$$

Calculate the change in stress $\Delta\sigma_z$ at the center of each layer using as an approximation Boussinesq stress distribution theory for a square foundation and the average applied stress, $\sigma(1)$:

$$\text{Layer 1: } z/B = 5 \text{ ft./13 ft.} = 0.38B; \Delta\sigma_z = I_z \cdot \sigma = 0.82 (2367 \text{ psf})$$

$$\Delta\sigma_z = 1941 \text{ psf}$$

$$\text{Layer 2: } z/B = 14 \text{ ft./13 ft.} = 1.08B; \Delta\sigma_z = I_z \cdot \sigma = 0.31(2367 \text{ psf})$$

$$\Delta\sigma_z = 734 \text{ psf}$$

The change in stress $\Delta\sigma_z$ calculated above is the average stress change over the unit cell.

Assume a stress concentration factor $n = 3$ (an n value less than 4 is used because the soil is relatively stiff compared with soft clays). The stress in the sandy silt from equation (8a) is

$$\mu_c = 1/[1 + (n-1) a_g] = 1/[1 + (2.0)(0.167)] = 0.750$$

The stress change in the clay as an approximation can be taken to equal $\mu_c \Delta\sigma_z$ giving the following settlements for Layers 1 and 2:

$$S_1 = \frac{0.06}{1+0.9} \log_{10} \left(\frac{960 \text{ psf} + 1941 \text{ psf} (0.750)}{960 \text{ psf}} \right) (10 \text{ ft. x 12 in.}) = 1.5 \text{ in.}$$

-
1. For a discussion of stress distribution and charts, tables, etc. for calculating changes in stress due to foundation loadings, refer to standard textbooks on soil mechanics [c.f., 62, 65, 74, 88].

$$S_2 = \frac{0.08}{1+1.0} \log_{10} \left(\frac{1810 \text{ psf} + 734 \text{ psf} (0.750)}{1810 \text{ psf}} \right) (8 \text{ ft.} \times 12 \text{ in.}) = 0.44$$

The total settlement in the sandy silt strata is about $S_t = 1.9$ in. Had stone columns not been used, the settlement would have been $S = 2.4$ in., giving $S_t/S = 1.9/2.4 = 0.79$. From equation (22), $S_t/S \geq \mu_c = 0.75$, which illustrates that $S_t/S \approx \mu_c$ is a quite useful approach for preliminary estimates of the level of reduction of settlement for various stone column designs. In the above simplified equation the variables affecting the settlement ratio S_t/S are only a_s and n .

Stress distribution can also be approximately considered using the finite element design charts. To do this an average stress σ is calculated within the compressible layer and used in the chart rather than the stress actually applied at the top of the layer.

Time Rate of Primary Consolidation. In Settlement Example 2, only four stone columns are used. Also, two layers of sandy silt are present which would have different coefficients of consolidation. Assume c_v (and c_{v_r}) in one layer differs from c_v (and c_{v_r}) in the other layer by a factor of about 2 to 5. For the resulting complex three-dimensional flow conditions, a theoretically accurate evaluation of the time rate of settlement for this problem would be a major undertaking. Such a solution would require a three-dimensional numerical analysis. As a rough, engineering approximation, however, the following simplified approach can be taken:

1. Consider for each layer radial and vertical flow separately and use equation (25) to estimate the combined results.
2. For radial flow neglect any interaction between the two layers. Sketch in the approximate radial flow paths on a scale drawing (Fig. 100). Remember that flow originates from lines of geometric symmetry and moves approximately radially to the drains.

Consider the flow to the drain shown in the upper lefthand corner of Fig. 100. An examination of the flow paths on the figure show 25 percent of the flow to the stone column from quadrant a-o-b is from infinity. This means D_e for this quadrant is very large, and from equation (28) the radial time factor $T_r = 0$. Over quadrants b-o-c and a-o-e, which together comprises another 25 percent of the drain, the flow path length varies from infinity at points b and a to short drainage paths at points c and e; this combined quadrant will only be partially effective in providing drainage. Finally, the area contributing flow to the drain that lies to the right and below line c-o-e has short flow paths that can be approximated by an estimated equivalent unit cell diameter $D_e \approx 7.5$ ft. shown in dashed lines on the figure. As an engineering approximation for this example,

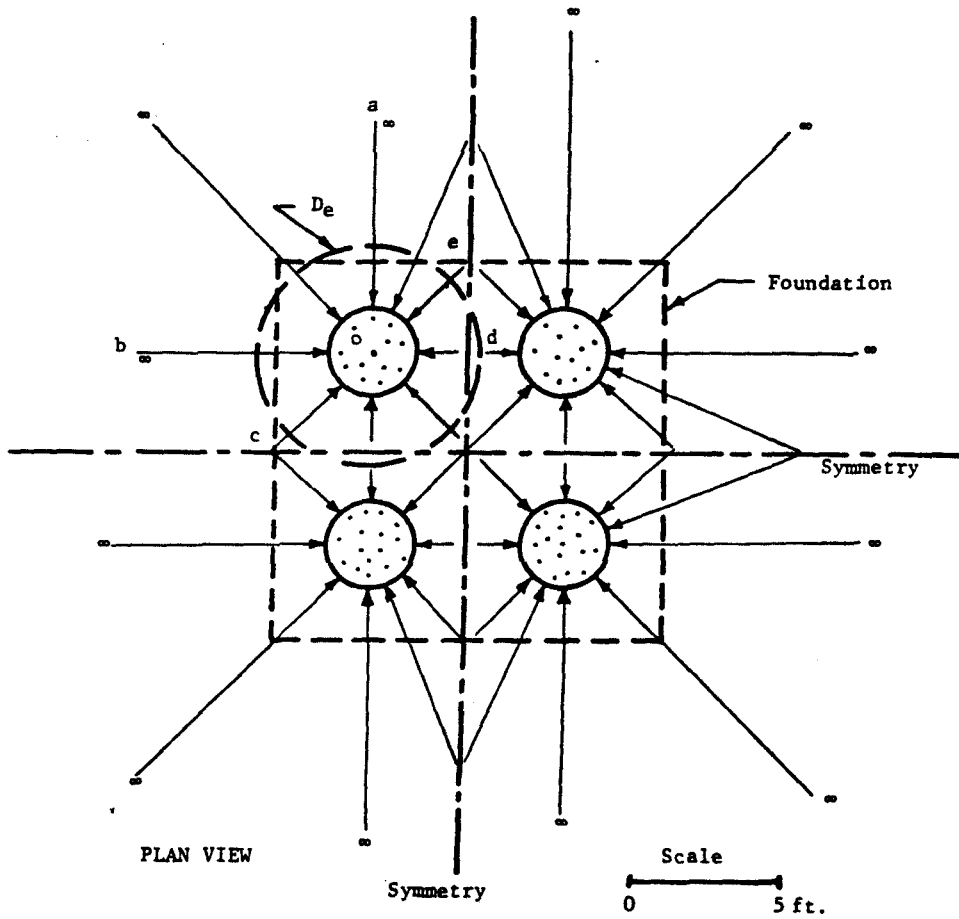


FIGURE 100. APPROXIMATE RADIAL FLOW PATHS FOR SETTLEMENT EXAMPLE 2.

estimate the time factor T_r for each layer using the appropriate value of c_{v_r} and $D_e \approx 7.5$ ft. To crudely consider that D_e effectively is very large over between 25 to 50 percent of the drain, reduce the time factor by about $(25\% + 50\%)/2 = 37.5\%$ or 0.4 (multiply the calculated time factor T_r by 0.6 or use 0.5 to be a little more conservative).

To illustrate this approximate approach assume for Layer 1 $c_{v_r} = 5c_v$ and $c_v = 0.2$ ft.²/day. Then at the end of 2 months the radial time factor would be estimated from equation (28) as $T_r = c_{v_r} \cdot t / D_e^2 = 5(0.2 \text{ ft.}^2/\text{day})(2 \times 31 \text{ days}) / (7.5 \text{ ft.})^2 = 1.10$. Reducing the time factor to approximately consider partial drainage gives $T_r = 0.5(1.10) = 0.551$. Assume the stone column diameter is effectively reduced by 1/5 to account for smear, giving from equation (29a) $n_{equiv}^* = 7.5 \text{ ft.} / (3 \text{ ft.} \times 0.2) = 12.5$. Then from Fig. 43 the degree of radial consolidation $U_r = 0.91$. Conservatively neglecting vertical drainage in Layer 1, the settlement after 2 months of Layer 1 is $S \approx 1.5$ in. $(0.9) = 1.35$ in. As would be expected, consolidation occurs rapidly in the sandy silt.

3. Since in this example $c_{v_r} = 5 c_v$ for Layer 1, vertical compared to radial consolidation would be relatively slow, and was conservatively neglected. However, if the effect of vertical drainage on the time rate of consolidation is desired, the presence of two layers greatly complicates vertical time rate of consolidation computations. If c_v of the more permeable layer is more than 20 times c_v of the less permeable layer, the following simplified approach can be used [62, p.415]:
 - (1) Assume consolidation occurs in two stages, (2) In Stage 1, calculate consolidation of the more permeable layer, assuming no drainage at the interface between the two, (3) In Stage 2 calculate consolidation in the least permeable layer, assuming drainage at the interface. If c_v of one layer is less than 20 times c_v of the other, the approximate method described in NAVFAC DM-7 [86] can be followed or numerical methods can be used [62, p.415].
4. Commentary. The above methods are, of course, quite crude and should be considered "ball park" in accuracy. They do give a rational way of approaching a very complicated, three-dimensional time rate of primary consolidation problem.

APPENDIX E
EXAMPLE STABILITY PROBLEM

This example illustrates how to handle the geometric and material parameters required for setting up a slope stability problem for analysis using the Profile Method described in Chapter III.

A 15 ft. (4.6 m) high embankment is to be placed over a soft clay as illustrated in Fig. 101. Because of the low shear strength of the soft clay use a stress concentration factor n of 2.0, and an angle of internal friction ϕ_s of the stone column of 42° . The saturated unit weight of the stone is 125 pcf (19.6 kN/m^3). For the first trial design, use 5 rows of stone columns laid out as shown in Fig. 101. An equilateral triangular grid will be used having a trial spacing $s = 6.5 \text{ ft. (2 m)}$. The stone column diameter is estimated to be 3.5 ft. (1.07 m) giving an area replacement ratio of

$$a_s = 0.907 (3.5/6.5)^2 = 0.263 \quad (5b)*$$

The plan view of the stone column grid used to improve the site is shown in Fig. 101(b). As shown in the figure, stone columns replace only 26 percent of the total volume of the soft clay (i.e., $a_s = 0.263$). Further, in performing a conventional stability analysis, the materials are assumed to extend for an infinite distance in the direction of the embankment. Typically the analysis is then performed on a 1 ft. (0.3 m) wide slice of embankment. To use the profile method the discrete stone columns must therefore be converted into equivalent stone column strips extending along the full length of the embankment as follows:

$$A_s = \pi D^2/4 = 3.14 (3.5 \text{ ft.})^2/4 = 9.62 \text{ ft.}^2$$

The length tributary to each stone column in the direction of the embankment is $s = 6.5 \text{ ft. (2 m)}$. Therefore a solid strip having the same area and volume of stone would have a width w of

$$w = A_s/s = 9.62 \text{ ft.}^2/6.5 \text{ ft.} = 1.48 \text{ ft.}$$

The total width of the tributary area equals

* These numbers refer to equations previously given in the main text.

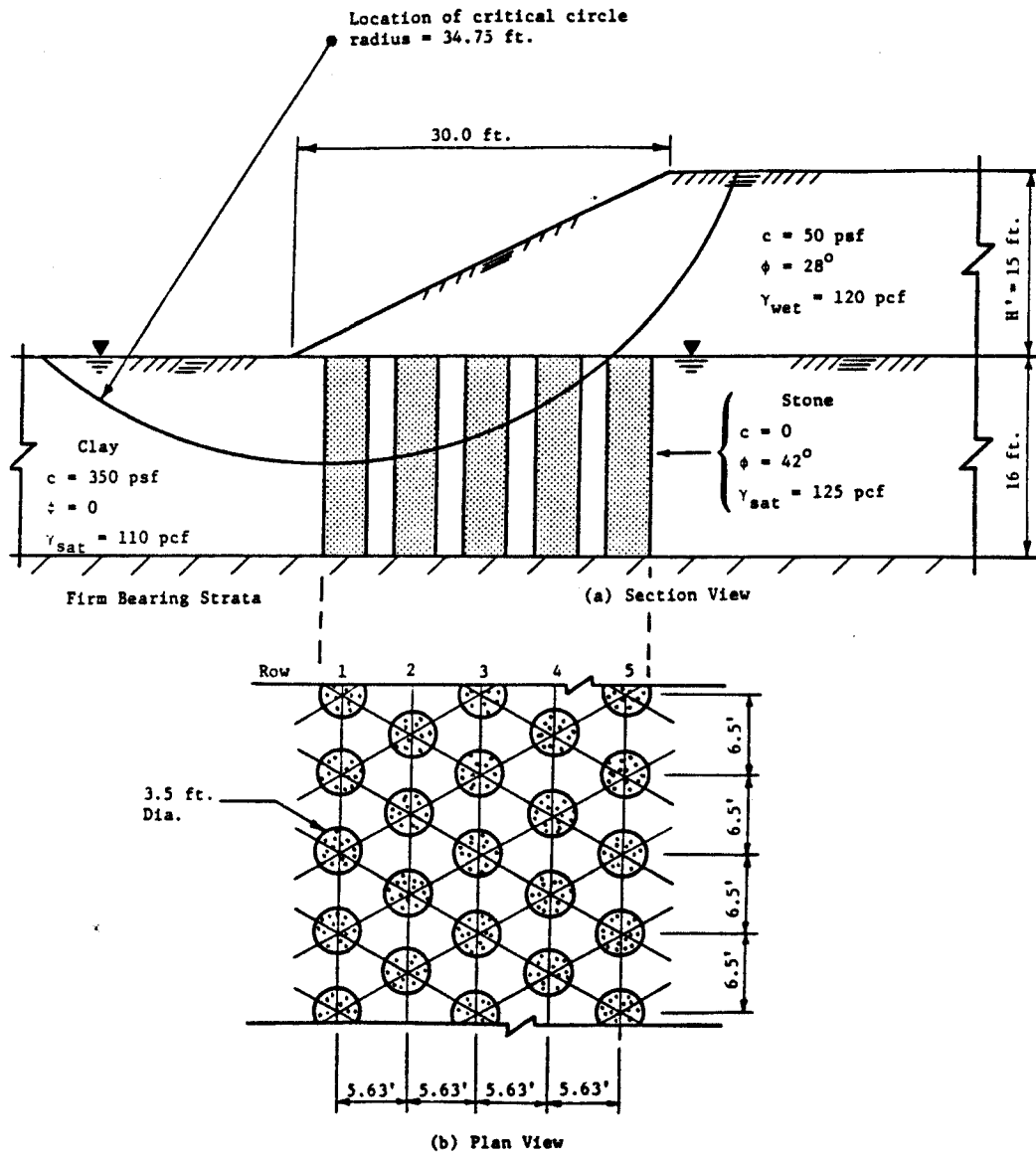


FIGURE 101. STABILITY EXAMPLE PROBLEM 1.

$A_s/(a_s s) = 9.62 \text{ ft.}^2 / (0.263 \times 6.5 \text{ ft.}) = 5.63 \text{ ft.}$ which is the stone column spacing 0.866s in the direction perpendicular to the embankment length.

Now determine the characteristics of the fictitious strips that must be added to handle the effect of stress concentration in the stability analysis. Let the thickness \tilde{T} of a fictitious strip be 0.3 ft. (91 mm) under the full embankment. Note that in this example no stone columns are actually used under the full embankment height for the first trial. However, stone column row 5 is located so that the edge of the tributary area is just at the break in the embankment. Therefore the unit weights calculated for the full embankment height can be used for each strip, with the thickness of the strips varying from zero at the toe to 0.3 ft. (91 mm) at the break (Fig. 102). An examination of equations (33) and (34) shows that this method gives the proper stress concentration in each strip. The thickness of the boundaries of each zone is calculated in Table 15.

The unit weights to use in the fictitious strips are calculated as follows:

$$\mu_s = n/[1 + (n-1) a_s] = 2.0/[1 + (0.263)] = 1.58 \quad (8b)^*$$

$$\mu_c = 1/[1 + (n-1) a_s] = 1.0/[1 + (0.263)] = 0.792 \quad (8a)^*$$

The correct unit weight to use above each stone column in the fictitious strip is

$$\begin{aligned} \gamma_f^s &= (\mu_s - 1) \gamma_1 H' / \tilde{T} = (1.58 - 1)(120 \text{ pcf}) 15 \text{ ft.} / 0.3 \text{ ft.} \quad (33)^* \\ &= 3480 \text{ pcf} \end{aligned}$$

and the unit weight to use above the soil in each fictitious strip is

$$\begin{aligned} \gamma_f^c &= (\mu_c - 1) \gamma_1 H' / \tilde{T} = (0.792 - 1) 120 \text{ pcf} (15 \text{ ft.}) / 0.3 \text{ ft.} \quad (34)^* \\ &= -1248 \text{ pcf} \end{aligned}$$

Material Properties and Zones are as follows (refer to Fig. 102):

$$\text{Zone 1: } \gamma_w = 120 \text{ pcf, } c = 50 \text{ psf, } \phi = 28^\circ$$

$$\text{Zone 2: } \gamma_w = 0, \quad c = 0, \quad \phi = 0$$

$$\text{Zones 3,5,7,9,11,13: } \gamma = -1248 \text{ pcf, } \phi = 0, \quad c = 0$$

TABLE 15. THICKNESS OF FICTITIOUS STRIPS.

Location	z (ft.)	$(30-z)$ (ft.)	Thickness, T_i , $0.01(30-z)$ (ft.)
T_1	0	30	0.300
T_2	2.07	27.93	0.279
T_3	3.55	26.45	0.265
T_4	7.70	22.30	0.223
T_5	9.18	20.82	0.208
T_6	13.33	16.67	0.167
T_7	14.81	15.19	0.152
T_8	18.96	11.04	0.110
T_9	20.44	9.56	0.096
T_{10}	24.59	5.41	0.054
T_{11}	26.07	3.93	0.039
T_{12}	28.15	1.85	0.018

T_i = Thickness of Fictitious Layer at Location shown on Fig.102.

Zones 4,6,8,10,12: $\gamma = +3480$ pcf, $\phi = 0$, $c = 0$

Zones 14,16,18,20,22,24: $\gamma_{\text{sat}} = 110$ pcf, $\phi = 0$, $c = 350$ psf

Zones 15,17,19,21,23: $\gamma_{\text{sat}} = 125$ pcf, $\phi = 42^\circ$, $c = 0$

The calculated safety factor of the slope is shown in the table below for the following conditions: (1) no improvement with stone columns, (2) the stone column improvement shown in Fig. 101 using a stress concentration factor $n=1$, and (3) the same level of improvement with $n=2.0$ (the critical circle for this condition is shown in Fig. 101). A simplified Bishop analysis was performed using the GTICES Lease II computer program [122].

Case	n	Coordinate (1)		R (ft.)	S.F.	Comment
		x (ft.)	y (ft.)			
1. No S.C. ⁽²⁾	-	14.20	27.00	43.00	1.07	Base Failure
2. S.C.	1	2.90	26.00	42.00	1.38	Base Failure
3. S.C.	2.0	2.90	26.00	34.75	1.65	See Fig. 101

Notes: 1. Coordinates of critical circle (refer to Fig. 101 for location of x and y axes).

2. Notation: S.C. = stone column; S.F. = safety factor;
R = radius of critical circle

APPENDIX F

RAMMED FRANKI STONE AND SAND COLUMNS

INTRODUCTION

Rammed stone and sand columns are constructed by the Franki Company primarily in Belgium and West Germany using a technique essentially the same as for the Franki pressure injected footing (concrete pile) [107,108]. Franki also constructs stone columns using a hydraulic vibrator following usual vibro-replacement construction procedures. The hydraulic vibrator used by Franki for vibro stone columns develops 111 H.P. (83 kw) and a centrifugal force of 38 tons (341 kN) at a frequency of 2500 rpm.

Franki rammed stone or sand columns are primarily used to support warehouses, including the floor slab, footings or slabs of low, multiple story buildings, tanks, tunnels through embankments, and stockpiles of raw materials. In these applications the main purpose is to limit total and differential settlement. Rammed stone columns are also sometimes used to increase the safety factor against sliding of a slope or to limit the horizontal soil displacement caused by surcharge loading by a raw material stockpile. This application reduces the passive bending pressure on piles supporting nearby structures.

The primary advantages of rammed stone columns over the conventional vibro method appears to be as follows: (1) The hole is cased using the Franki method and one method used by Datye, et al. [53]. As a result possible hole collapse is avoided in soft clays and cohesionless soils having a high groundwater table. Also stone is not dropped down an uncased hole. (2) Either sand or stone can be used with the Franki method. (3) Jetting and flushing water is not required. (4) Problems with soil erosion during flushing are avoided in organic soils and peat.

The main disadvantage of rammed stone columns is that the time required to construct the column is, for some applications, greater than for vibro methods. Also, driving the casing causes smear along the sides of the hole that reduces the radial permeability of the soil (refer to Fig. 56). Because of the high level of ramming used in the construction process, large excess pore pressures are created in the surrounding, low permeability cohesive soil. The excess pore pressures, however, reportedly dissipate rapidly resulting in rapid consolidation and strength gain. If a coarse, open graded stone is used, however, clogging may occur reducing the effectiveness of the stone column to act as a vertical drain. Also, for some applications such as slope stabilization, development of large excess pore pressures would be undesirable. A reduced level of energy input could be used to minimize this problem.

CASE HISTORIES

Tunnel Support

To limit settlement, a 13 ft. (4 m) wide tunnel was founded on four rows of rammed, coarse sand columns at Deinze, Belgium. The tunnel crosses through a 23 ft. (7 m) high compacted fill which applies a pressure of 2.5 ksf (125 kN/m²) to the original soil at the base of the tunnel (Fig.103). The fill supports five railway lines. The load on the sand columns is mainly due to negative friction transmitted by the fill to the vertical exterior faces of the tunnel.

The sand columns have a 6.6 ft. (2 m) spacing on a square pattern. They are 2.1 ft. (0.64 m) in diameter and were constructed using a 17.7 in. (0.45 m) casing. The tips of the columns are founded in a dense sand layer at a depth of 57 ft. (17 m). Normally consolidated, loose silty sands of Quaternary age overly the dense sand. A stratum of stiff clay of Tertiary age is found beneath the dense sand. The measured cone resistance before construction is shown in Fig. 103 as a function of depth.

Composite Gravel-Concrete Column

Composite rammed Franki gravel and concrete columns were constructed in 1976 to 1977 at the Beaver Valley Nuclear Station at Shippingport, Pennsylvania. The columns were used to densify a loose sand layer susceptible to liquefaction during an earthquake. The loose sand layer is located from a depth of 35 to 80 ft. (10.7-24.4 m) below the surface. Dense coarse sands and gravels overlay the loose sand.

The columns were constructed with a 21 in. (0.535 m) diameter casing using a 7.5 ft. (2.28 m) spacing in a triangular pattern. The columns were constructed through the loose sand stratum by ramming successive expanded bases or dry, lean concrete using a 3 ft. (0.9 m) vertical driving interval. Sand and gravel shafts were used above in the dense sands and gravels.

In the loose zone successive bases were built using 140,000 ft-lb blows (1.9 MN-m) up to a specified number of blows per 5 ft.³ (0.14 m³). The consumption of dry concrete was about 15 ft.³ (0.42 m³) per base. Although the primary purpose of the columns was to densify the loose sand, use of concrete to construct these columns also stiffened the stratum.

CONSTRUCTION

Rammed Franki stone or sand columns are generally constructed using 16, 18, 20.5 and 24 in. (400-600 mm) diameter casing. The casing is driven to the specified depth, usually by hammering on a temporary stone or sand plug located at the bottom of the casing. A 3 to 4.5 ton ram is used in construction, which is the same as for the Franki concrete pile. The height of fall, usually 13 to 20 ft. (4-6 m), is chosen considering the soil strength

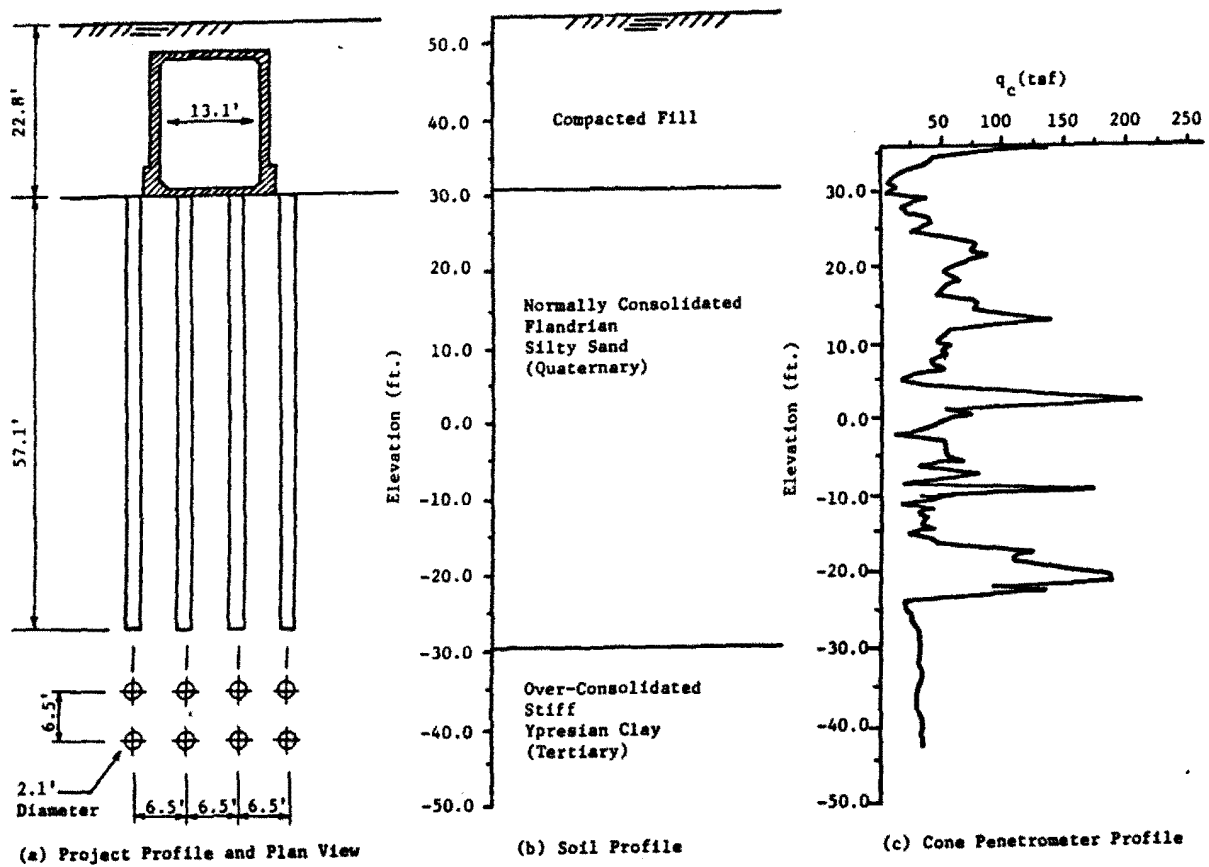


FIGURE 103. USE OF RAMMED STONE COLUMNS FOR TUNNEL SUPPORT AT DEINZE, BELGIUM.

and project requirements.

When the specified depth is reached, the plug is driven out by hammering with the casing maintained in position or slightly pulled up by tension ropes. The stone or sand column is constructed by ramming about 3.5 ft.³ (100 liters) of material in successive lifts as the column is brought up. As the column is constructed, the casing is progressively extracted. The diameter of the compacted column is determined by the effective volume of material used per unit column length. The density of the granular column increases as the completed diameter of the column, compared to the casing, increases. The increase in diameter is usually between 4 in. (10 cm) and 12 in. (30 cm). Columns having a 36 in. (90 cm) diameter are routinely constructed with a 24 in. (60 cm) casing, and 32 in. (80 cm) diameter columns with a 20.5 in. (52 cm) casing. Since the soil to be improved with stone or sand columns in general is not very stiff, columns can be constructed with diameters greater than 48 in. (1.2 m). Franki has constructed concrete bases up to 60 in. (1.5 m) in diameter in both loose sandy and stiff clayey soils.

Depending on the soil strength profile, the following three methods can be used to construct Franki rammed columns.

1. The easiest and most certain technique is to construct a column with a constant diameter. This method requires varying the energy applied depending upon the soil strength.
2. A second approach is to increase the volume of material over the required volume as long as a critical value of energy per unit length of column has not been developed. As a result, the column diameter changes with the soil strength. The problem with this method is in determining the required critical compaction energy level. The best approach is to use field tests comparing profiles of, for example, measured cone resistance, and the energy per unit length required to develop columns of various diameters. To avoid problems a certain minimum length of plug should be maintained throughout driving. This minimum plug length must be the largest necessary length for any stratum to prevent soil or water from entering into the casing. Sometimes this requirement is expensive, and the benefit resulting from the diameter of the column changing with the soil strength is lost compared to a column having a uniform diameter; the diameter of a uniform column would be the largest necessary to limit settlement to an acceptable level.
3. A practical alternative which is easier to construct and more reliable than the constant energy method (Alternative 2) is to develop a stepped diameter column. Consider when a column having an insufficient diameter is formed through a soft layer. Following the stepped column approach, the casing is plugged and redriven through the completed column to the bottom of the soft layer. A second column, lying on the axis of the first, is then constructed upward to obtain the required diameter in that stratum.

Using experience gained with zero slump concrete Franki piles, the volume of rammed stone or sand columns is assumed for preliminary estimates to be 0.8 the loose volume. During construction of the column, the length of the granular plug remaining in the bottom of the casing is never allowed to get small enough to let soil or water to enter the casing. Stone columns are generally constructed using rounded material having a maximum size of 1.2 to 2.4 in. (30-60 mm). When necessary, as for concrete piles, the base of the column can be enlarged.

With the available equipment and customary stone column diameters used, a production rate of 400 to 660 ft. (120-200 m) of column is usually obtained per 8 hour shift, depending on the soil strength.

DESIGN

Franki stone columns are always carried down to firm bearing material. Design column loads vary from 20 to 60 tons. A stone column spacing of 3 diameters is usually employed with the minimum being 2.5 diameters. For coarse stone an angle of internal friction up to 45° to 50° is used for stability analyses. For sand an angle of internal friction less than 40° is used. The larger values of the angle of internal friction requires a well densified material. A column is considered to be well densified if the diameter of the column is equal to or greater than the diameter of the casing plus 4 in. (10 cm).

The deformation and the bulging load of a single column are estimated from Menard pressuremeter test results, or from Vesic cavity expansion theory (refer to Chapter III). For large groups of columns, the latter theory is modified to take into account the fact that the radius of influence of the columns is limited, and the vertical stresses are increased by the surcharge transmitted at the soil surface. A coefficient of at-rest earth pressure K_0 less than one is used along the zone of influence.

Two different type settlement analyses are made when (1) the stiffness of the slab transmitting the loads does not permit differential settlement to occur between the column and the soil (equal strain assumption), and (2) the transmitting element is flexible, i.e., the settlement of the soil is larger than settlement of the columns. The modulus of elasticity of the soil is obtained from the results of laboratory consolidation tests, cone penetration tests, or pressuremeter tests. Drained soil response is used to consider long-term effects.

For columns loaded between about 20 and 30 tons, the settlement is usually between approximately 0.4 and 0.8 in. (10-20 mm). In low permeability soils where high excess pore pressures are anticipated, a sand is usually preferred to prevent clogging. Clogging would reduce the rate of water flow vertically through the column resulting in a greater length of time for the soil to consolidate and gain strength. Sand, which is also used when gravel is not available or is too expensive, is believed to result in more settlement than stone [51.]

FIELD INSPECTION

When the required diameter is constant over the length of the column, field inspection is conducted by estimating the diameter of the stone or sand column. Therefore, the quantity of material consumed during construction is measured per unit of length of column, and the diameter calculated. When a critical energy per unit of length is specified in addition to a minimum diameter, both the quantity of material added and the energy used are measured per unit of column length.